A NOVEL RADIO RESOURCE MANAGEMENT TECHNIQUE FOR INTERFERENCE MANAGEMENT IN LTE-A HETEROGENEOUS NETWORKS

A THESIS SUBMITTED TO
GRADUATE SCHOOL OF NATURAL AND APPLIED SCIENCES
OF
KOCAELI UNIVERSITY

BY

SAJJAD AHMAD KHAN

IN PARTIAL FULFILLMENT OF THE REQUIREMENTS
FOR
THE DEGREE OF DOCTOR OF PHILOSOPHY
IN
COMPUTER ENGINEERING

KOCAELI 2019

A NOVEL RADIO RESOURCE MANAGEMENT TECHNIQUE FOR INTERFERENCE MANAGEMENT IN LTE-A HETEROGENEOUS NETWORKS

A THESIS SUBMITTED TO
GRADUATE SCHOOL OF NATURAL AND APPLIED SCIENCES
OF
KOCAELI UNIVERSITY

BY

SAJJAD AHMAD KHAN

IN PARTIAL FULFILLMENT OF THE REQUIREMENTS
FOR
THE DEGREE OF DOCTOR OF PHILOSOPHY
IN
COMPUTER ENGINEERING

Prof. Dr. Adnan KAVAK
Supervisor, Kocaeli University .....

Prof. Dr. Vedat COŞKUN
Jury member, Beykent University .....

Assoc. Prof. Dr. Kerem KÜÇÜK
Jury member, Kocaeli University .....

Assoc. Prof. Dr. Cüneyt BAYILMIŞ
Jury member, Sakarya University .....

Assist. Prof. Dr. Sultan ALDIRMAZ ÇOLAK
Jury member, Kocaeli University .....

Thesis Defense Date: 28.11.2019

ACKNOWLEDGMENT

Firstly, I would like to express my gratitude and reverence to ALLAH Almighty, who gives me strength, ability, knowledge, and patience to continue my research studies as well as the perseverance to complete my doctorate satisfactorily. I believe that without His blessings, it has not been possible.

I wish to express my sincere gratitude and warmest thanks to my supervisor, Prof. Dr. Adnan Kavak for his continuous support, guidance, motivation, and supervision throughout my doctorate studies. His professional approach and practical knowledge helped me to complete my doctorate in the best possible way. It wouldn't be possible without his great support. I'm also very thankful to his family for considering me as their family member.

I take pride in acknowledging the insightful guidance of Assoc. Prof. Dr. Kerem Küçük who co-supervised me during my studies. I'm truly blessed and privileged to study under his guidance. I salute to his full support, invaluable guidance, motivation, and suggestions during my studies.

Along with, I am also grateful to Assist. Prof. Dr. Sultan Aldırmaz Çolak for her invaluable time, comments, suggestions and contributions to my research work. My big thank goes to Assoc. Prof. Dr. Cüneyt Bayılmış for being a permanent member of my jury. He always encouraged and gave me worthy suggestions. I'm very thankful to Prof. Dr. Vedat Coşkun for being a senior member of my thesis committee. His valuable comments and suggestions improved the quality of my thesis.

Besides my professors, I am really thankful to all my friends especially Dr. Muhammad Asshad, who always supports me in every situation of my life. I am also very thankful to all the academic personnel of the Computer Engineering Department at Kocaeli University, Turkey.

Last but not least, I am obliged to my Parents Mr. Kamil Ghulam Khan and Zara Khatoon for their unconditional love, support and prayers. I'm very much thankful to my brothers and sisters for their love and support.

November, 2019 Sajjad Ahmad Khan

CONTENTS

LIST OF FIGURES

LIST OF TABLES

LIST OF SYMBOLS AND ABBREVIATIONS

PL	: Path Loss
M	: Macrocell
F	: Femtocell
ω	: Total number of RBs
K	: Total number of subbands
S	: Total number of cell sectors
L	: Total number of cell layers
SB	: Set of subbands
Ω	: Set of subbands in each sector
$G^{k}_{m,M}$	: Channel gain between macrocell M and MUE m at subcarrier k
$G^{k}_{f,F}$	: Channel gain between femtocell F and FUE f at subcarrier k
$SINR^{k}_{m}$	: SINR value received by MUE m at subcarrier k
$SINR^{k}_{f}$	: SINR value received by FUE f at subcarrier k
P^{k}_{M}	: Transmit power of macrocell M at subcarrier k
P^{k}_{F}	: Transmit power of femtocell F at subcarrier k
N_o	: White noise power density
Δf	: Center frequency
P_{tx}	: Macrocell transmit power for each layer
C^{k}_{m}	: Capacity achieved by MUE m at subcarrier k
C^{k}_{f}	: Capacity achieved by FUE f at subcarrier k
Υ_{rx}	: Min. detectable RSRP (dB) at the edge of each layer
φ^{M}_{i}	: Set of frequencies received at femtocell (F_i) from macrocells (M)
φ^{F}_{i}	: Set of frequencies received at femtocell (F_i) from other femtocells
T_X	: Throughput achieved by femtocell F or macrocell M
T_{total}	: The overall throughput achieved whether by all UEs
λ	: Group of usable SBs for femtocell (F_i) in a sector
\	: Indicates exclusion in set theory
$\zeta^{F}_{i,j}$	: Group of frequencies received from femtocells of other sectors
ψ^{k}_{x}	: Notifies the assignment of subcarrier k to UEs x
$\varphi^{F}_{i,j}$	: Group of frequencies received from other femtocells of the same sector
$\varphi^{assigned}_{i}$	: The assigned frequency SB to the femtocell (F_i)
η	: Efficiency achieved by the system
ρ	: Ratio of user distribution in the central layer
Γ_{thr}	: SINR threshold
q	: Ratio of central layer radius to cell radius
N_{UE}	: Total Number of UEs in a cell

Abbreviations

1G	: First Generation
2G	: Second Generation
3G	: Third Generation
3GPP	: Third Generation Partnership Project
4G	: Fourth Generation
5G	: Fifth Generation
ADSL	: Asynchronous Digital Subscribers Line
AMPS	: American Mobile Phone System
AP	: Access Point
ARRM	: Adaptive Radio Resource Management
BW	: Bandwidth
CCI	: Co-Channel Interference
CDMA	: Code Division Multiple Access
CLF	: Central Layer Focus
CP	: Cyclic Prefix
CQI	: Channel Quality Indicator
CRC	: Cyclic Redundancy Reference
CRS	: Cell Specific Reference
DL	: Downlink
EDGE	: Enhanced Data Rates for GSM Evolution
eNB	: evolved Node Base Station
EPC	: Evolved Packet Core
EUTRAN	: Evolved-UMTS Terrestrial Radio Access Network
FBS	: Femto Base Station
FC	: Femtocell
FDD	: Frequency Division Duplex
FDMA	: Frequency Division Multiple Access
FFR	: Fractional Frequency Reuse
FFR-3	: Fractional Frequency Reuse with Three Sectors
FFR3R	: Fractional Frequency Reuse with Three Regions
FFR3SL	: Fractional Frequency Reuse with Three Sectors and Three Layers
FFT	: Fast Fourier Transform
FUE	: Femtocell User Equipment
GPRS	: General Pocket Radio Service
GSM	: Global System for Mobile Communication
HeBN-GW	: HeNB Gateway
HeNBs	: Home Evolved Node Base Station
HetNets	: Heterogeneous Networks
HSDPA	: High Speed Downlink Packet Access
HSDPA	: High Speed Downlink Packet Access
HSPA	: High Speed Packet Access
HSUPA	: High Speed Uplink Packet Access
ICI	: Inter Carrier Interference
IFFT	: Inverse Fast Fourier Transform
IMT	: International Mobile Telecommunication

IMT-A : International Mobile Telecommunication Advanced
IoT : Internet of Things
IP : Internet Protocol
ISI : Inter Symbol Interference
ITU-R : International Telecommunication Union Radio Communication
KPI : Key Performance Indicator
LTE : Long Term Evolution
LTE-A : Long Term Evolution Advanced
MC : Micro Cell
MIMO : Multiple Input Multiple Output
MLF : Middle Layer Focus
MUE : Macrocell User Equipment
NMT : Nordic Mobile Telephone
OFDM : Orthogonal Frequency Division Multiplexing
OFDMA : Orthogonal Frequency Division Multiple Access
OLF : Outer Layer Focus
OSFFR : Optimal Static Fractional Frequency Reuse
PC : Pico Cell
PCA : Power Control Algorithm
PHY : Physical Layer
QAM : Quadrature Amplitude Modulation
QoS : Quality of Service
RAN : Radio Access Network
RB : Resource Block
RF : Radio Frequency
RLC : Radio Link Control
RRC : Radio Resource Control
RRM : Radio Resource Management
RSRP : Reference Signal Received Power
RSRQ : Reference Signal Received Quality
RSSI : Received Signal Strength Indicator
RTT : Round Trip Time
SAE : System Architecture Evolution
SC : Small Cell
SCOFDMA: Single-Carrier Frequency Division Multiple Access
SINR : Signal to Interference and Noise Ratio
SNR : Signal to Noise Ratio
TDD : Time Division Duplex
TDMA : Time Division Multiple Access
TTI : Transmission Time Interval
UE : User Equipment
UL : Uplink
ULD : User Location Distribution
UMTS : Universal Mobile Terrestrial System

LTE-A HETEROJEN AĞLARDA PARAZİT YÖNETİMİ İÇİN YENİLİKÇİ BİR RADYO KAYNAK YÖNETİM TEKNİĞİ

ÖZET

Yeni nesil kablosuz ağların ortaya çıkmasıyla birlikte, kablosuz abonelerin sayısı ve bu sistemlerin sağladığı yüksek veri hızının yanında farklı servislere olan ilgi her geçen gün katlanarak artmaktadır. Bununla birlikte, böylesi bir artış bu ağlardaki bilhassa LTE-A kablosuz ağların hedef özelliklerinden birisi olan Heterojen Ağlardaki (HetNet) radyo kaynaklarının verimli bir şekilde kullanılmasını gerektirir. HetNet, makro hücreler, mikro hücreler, piko hücreler, ve femto hücreleri barındıran çok katmanlı bir hücresel kablosuz ağdır. Bir HetNet'de ağ trafiği bazı optimizasyon kriterlerine, politikalara, vb. kriterlere göre bu farklı hücreler tarafından paylaşılır. Öte yandan, HetNet'ler için kritik zorluklardan birisi böylesi parazit sınırlı bir ortamda radyo kaynaklarının verimli bir şekilde kullanılmasıdır. Yakın zamanda, Parçalı Frekans Tekrar Kullanımı (FFR) LTE-A HetNet ağlarda eş-katman ve çapraz-katman parazitleriyle başa çıkmak ve sistem başarımını arttırmak için ön plana çıkan radyo kaynak yönetim tekniklerinden birisi olarak ortaya çıkmaktadır. Bununla birlikte, radyo kaynaklarını daha verimli kullanmak, daha yüksek başarım ve daha iyi spektral verimlilik elde etmek için, LTE-A HetNet'lere yönelik yeni RRM tekniklerine hala ihtiyaç bulunmaktadır.

Bu tezde, üç sektörlü ve üç katmanlı FFR (FFR-3SL) olarak adlandırdığımız, LTE-A HetNet'ler için yenilikçi bir RRM tekniği önermekteyiz. Önerilen FFR-3SL yönteminde, tüm makro hücre kapsama bölgesi merkez, orta, ve dış katmanlar olarak üç katmana ve ayrıca üç sektöre ayrıştırılmaktadır. Öte yandan, toplam mevcut bantgenişliği A, B, C, D, E, F ve G olarak yedi alt banta bölünmektedir. Alt bant 'G' yalnızca merkez katmandaki makro kullanıcılara tahsis edilirken, kalan altı alt bant ise makro kullanıcılar ve femto kullanıcılar tarafından kendilerine ayrılan bölgelerde paylaştırılmaktadır. Sonuçta, eş-katman ve çapraz-katman parazitleri ile öncelik durumuna göre başa çıkılmaktadır.

FFR-3SL yönteminin performansını, sistem başarımı, spektral verimlilik, kullanıcı memnuniyeti, vb. ölçütler açısından değerlendirmek için bilgisayar benzetimleri yapılmıştır. Önerilen FFR-3SL yönteminin performansı aynı zamanda literatürdeki mevcut FFR yöntemleri ile karşılaştırılmaktadır. Sonuçlar, önerilen yöntem ile mevcut yöntemlere göre daha yüksek başarım ve daha iyi spektral verimlilik elde edildiğini göstermektedir. Buna ilave olarak, sistem verimliliği sinyalin parazit ve gürültüye oranı (SINR) değerleri açısından kullanıcı memnuniyetine göre iyileştirilmektedir. Bu tezde, aynı zamanda kullanıcı konum dağılımının (ULD) ve merkez, orta, ve dış katmanlardaki kullanıcı yoğunluklarının FFR-3SL yöntemine olan etkileri incelenmektedir. Bu koşulların etkisini dikkate alan güncellenmiş FFR-3SL yöntemi sunulmaktadır.

Anahtar Kelimer: Bölünmüş Freksans Yeniden Kulanımı, Femto Hücre, Heterojen Ağlar, LTE-A, Radyo Kaynak Yönetimi (RRM).

A NOVEL RADIO RESOURCE MANAGEMENT TECHNIQUE FOR INTERFERENCE MANAGEMENT IN LTE-A HETEROGENEOUS NETWORKS

ABSTRACT

With the emergence of new generation wireless networks, the number of wireless subscribers and demand for different services along with high data rates provided by them are increasing exponentially each day. Such an increase, however, requires efficient utilization of radio resources in these networks, especially in Heterogeneous Networks (HetNets) which is one of the target specifications of Long Term Evolution Advanced (LTE-A) wireless networks. A HetNet is a multi-tier cellular wireless network including macrocells, microcells, picocells, and femtocells, and the network traffic is shared by these cells according to some optimization criteria, policy, etc. Though, one of the critical challenges for HetNets is the efficient utilization of radio resources in such an interference limited environment. Recently, Fractional Frequency Reuse (FFR) methods have appeared as one of the prominent Radio Resource Management (RRM) techniques for LTE-A HetNets to mitigate co-tier and cross-tier interferences and to increase system throughput. However, in order to efficiently use radio resources and to achieve higher throughput and better spectral efficiency in LTE-A HetNets, there is still a need for new RRM techniques.

In this thesis, we propose a novel RRM technique for LTE-A HetNets, referred to as FFR with Three Sectors and Three Layers (FFR-3SL). In the proposed FFR-3SL method, the entire macrocell coverage area is split into three layers as central, middle and outer layers and three sectors. On the other hand, the total available bandwidth is divided into seven subbands such as A, B, C, D, E, F, and G. The subband 'G' is allocated to the macro users in the zones of central layer while the remaining six subbands are shared among the macro users and femto users in their respective zones. As a result, co-tier and cross-tier interferences are managed on a prior basis.

Simulations are performed to evaluate the performance of the FFR-3SL method in terms of system throughput, spectral efficiency, and user satisfaction, etc. The performance of the proposed FFR-3SL method is also compared with the existing FFR methods in the literature. The results show that the proposed method achieves higher throughput and better spectral efficiency as compared to existing methods. Furthermore, the efficiency of the system is improved with regard to user satisfaction in terms of signal to interference and noise ratio (SINR) values. In this thesis, the effects of user location distribution (ULD) and the user densities in central, middle and outer layers on FFR-3SL method are also investigated. Modified FFR-3SL method is presented under these conditions.

Keywords: Fractional Frequency Reuse (FFR), Femtocell, Heterogeneous Networks (HetNets), Long Term Evolution Advanced (LTE-A), Radio Resource Management (RRM).

INTRODUCTION

After a tremendous growth of mobile devices such as smartphones, tablets, smart TVs, and other hand-held devices and the high reliance on social networks and other web-based applications, the demand for high data rates increased drastically [1]. Furthermore, the number of internet subscribers increases every year at a very high rate. For example, Cisco forecasts that the global mobile data traffic will grow from an annual rate of 87 Exabytes of the year 2016 to 587 Exabytes in 2021 [2]. Statistics show, that between 2016 and 2021 mobile traffic is expected to increase two times faster than fixed network traffic [3]. Due to the fast improvement in broadband and wireless communication industry, the heterogeneous networks (HetNets) emerge as one of the most promising developments toward realizing the target specifications of Long Term Evolution (LTE) and LTE-Advanced (LTE-A) networks.

Radio Resource Management (RRM) is one of the core research areas for the upcoming Fifth Generation (5G) cellular networks. Femtocell networks are considered to be a feasible option that can fulfill the demands of high-speed voice and data traffic for indoor users. It uses the services of the existing broadband infrastructure to connect to the operator's core network. The cellular network operators need to modify the existing single-tier macrocell network in order to provide the services of femtocells to their users. This drove the attention of Third Generation Partnership Project (3GPP) group to create the LTE cellular system, to achieve higher data rates and capacity to support those multimedia applications [4].

With the advent of Fifth Generation (5G) and other wireless communication systems, the demand for high data rates increased exponentially and it is expected that it will further increase due to the use of smartphones and data-hungry applications. The reason is that in 5G all home appliances and other electronic devices are being considered as part of the internet, which is known as the Internet of Things (IoT). After the explosive growth of subscribers, mobile network operators started to investigate new technologies to deploy for data-hungry applications. The growth in data-intensive

mobile services and applications such as web browsing, social networking, music, and video streaming has become a driving force for development of the next-generation wireless standards. As a result, new standards are being developed to provide higher data rates and network capacity necessary to support worldwide delivery of these types of rich multimedia applications.

3GPP LTE-A is a promising 4G technology dealing with the increasing data throughput requirements of the mobile cellular network. Due to huge growth of smartphones, tablets, and notebook, etc., the high Quality of Service (QoS) and ubiquitous connections are required. On the other hand, the numbers of subscribers are increasing dramatically, and global LTE subscriptions will reach up to nearly 4 billion in 2020. According to global LTE passed 1 billion subscriptions in 2015 and will reach up to 3.62 until 2020 [5]. Due to the explosive growth of users and multimedia services the main challenge for next-generation cellular networks is to oblige mobile data traffic by improving the capacity of the networks [6]. The present LTE-A system is based on a homogeneous network, where every single evolved Base Station (eNB) covers the whole cell, and each eNB uses similar transmission power levels, modulation techniques, access schemes, antenna patterns to offer QoS to the User Equipments (UEs) across the cell [7]. However, such deployment degrades the coverage and capacity of cell-edge users.

One approach solving the above-mentioned problems is to shrink the cells and to provide high data throughput and fulfill the increasing demand for cellular systems, but this approach is not economical [8]. Therefore, the deployment of Heterogeneous Network (HetNet) is more scalable and beneficial for both operators as well as users. This approach is expected not only to improve the broadband user experience but also to increase the coverage and capacity of the cell in a cost-effective manner [9]. Small cells can support wireless applications for homes and enterprises as well as metropolitan and rural public spaces. Due to the smaller coverage area, the same licensed frequency band can be efficiently reused multiple times within the small cells in a HetNet, thus improving the spectral efficiency per unit area and hence the capacity of the network. In a HetNet, small cells are envisioned as traffic off-loading spots in the Radio Access Network (RAN) to decrease the congestion in macrocells and enhance

the users' QoS experience [10].

When there are a huge number of femtocells deployed in HetNet system macrocells and femtocells have to share the same spectrum, thereby resulting in downlink and uplink Co-Channel Interferences (CCI). Specifically, downlink transmissions from the femtocell may cause strong interference at a nearby macrocell's UEs degrade the performance and even interrupt the received macrocell signal at the macrocell's UE. Hence, CCI is one of the major barriers to the successful coexistence of macrocell and femtocell.

In this thesis, we propose to use novel radio resource management to mitigate interferences in LTE-A HetNets. The main approach in our proposed solution is the Fractional Frequency Reuse (FFR) with three sectors and three layers, which is called FFR-3SL. In FFR-3SL, the whole macrocell coverage area is segmented into three sectors and three layers, which become nine zones in a typical macrocell region. The available bandwidth is divided into seven small fractions of subbands referred to as radio resources. An algorithm to manage radio resources within the FFR-3SL concept is proposed. In order to improve the performance of the LTE-A HetNet system, FFR-3SL algorithm is further improved by taking user location distribution (ULD) into account.

The thesis is organized as follows: In Chapter-1, the background studies and motivation of this thesis are provided. Chapter-2 describes the general idea of LTE-A HetNet, basic architecture, and characteristics in detail. In Chapter-3, Fractional Frequency Reuse (FFR) Method for Resource Management in LTE-A HetNets is demonstrated and a novel proposed FFR-3SL method and its algorithm are explained. Chapter-4 presents the effect of user location and density on the proposed method. In Chapter-5, A Transmit Power Control (TCP) algorithm and software tool are given. Conclusion and future directions are discussed in Chapter-6.

1. BACKGROUND AND MOTIVATION

1.1. Evolution of Mobile Communication Systems

We are living in an era where every person is connected with the whole world through the internet and can access data anything from anywhere in less than a second. Everyone wants to share his personal data such as messages, voice, images, and videos, etc. with other friends and communities via social websites while traveling [11]. In addition, most of the automobiles and home appliances will also be connected to the internet in the near future [12]. In such a way, the number of mobile subscribers is growing with every passing day and it is expected that this number will reach up to 50 billion in 2020 [13]. In order to provide wireless internet services to everything, every time and everywhere the internet service providers always searching for better solutions and techniques. Currently, there are many options available which provide wireless connectivity to the internet; however, the best solution is the mobile cellular communication concept which offers wireless internet services to the users everywhere and every time [14]. As the number of users grows, the technologies become more complex. Recently, the Fifth Generation (5G) trials have been started to launch in some parts of the world. However, reaching up to 5G evolution took almost 40 years and it will provide extremely high data rates, faster response times and increasingly fluent means to access more content than ever in the history of telecommunications [15]. The history of the mobile network generations and the technologies are explained in Table 1.1.

Table 1.1. The evolution of wireless generations

Generation	**Peak Data Rate**	**Technology**	**Services**
1G	2.4 Kbps	Analog	Basic voice service
2G	64 Kbps	Digital standards (GSM, CDMA)	Designed for voice, Improve coverage and capacity
3G	2 Mbps	UMTS, OFDM based LTE	Voice with some data (multimedia, text, internet) First broadband service
4G	100 Mbps	OFDMA based LTE-A MIMO	VoIP, Data High speed broadband
5G	1 Gbps	IoT, mmWave Massive MIMO	Enhanced Mobile Broadband Smart Homes, Smart Cities High-definition Video Virtual Reality (VR), etc.

The first mobile cellular communication systems were launched by the Nordic Mobile Telephone (NMT) and the American Mobile Phone System (AMPS) in 1981 and 1982, respectively. These analog-based wireless communication systems used Frequency Division Multiple Access (FDMA) technology and called as First Generation (1G) systems [16]. The 1G systems provided services only for wireless voice communication with a speed of about 2.4 Kbps [17]. The limitations of 1G included large cell sizes, heavy mobile devices, expensive, less Quality of Service (QoS), low speed, and waste of frequency spectrum. Besides, users were facing problems when they moved away from the transmitter [18].

Due to these limitations, the mobile network operators started offering wireless digital communications to their subscribers in early 1990. It wouldn't be wrong if we say that second-generation (2G) was the real beginning of the current version of mobile cellular

technology. Unlike the analog system, the communications started in a digital form and carried with a narrow-band system [19]. Therefore, the was no interference problem, and it was easier to carry data. Data transfer rates in which telephony processors at that time could not cope gradually increased in the next generations with the development of the processors. In 2002, a General Pocket Radio Service (GPRS) was launched for data communication, and this technology was called as 2.5G; during this transition period, whose data rates enhanced up to 114 Kbps [20]. Even later, Enhanced Data Rates for GSM Evolution (EDGE) technology was called as 2.75G [21].

In 2004, the third-generation (3G) was launched and introduced extra features such as accessing the internet through portable devices, video calling, and video inspection, etc. [22]. The Universal Mobile Telecommunications System (UMTS) technology was introduced in 3G by using the same GSM standards. With 3G, the communication speed reached up to 2 Mbps [23]. Around 2006, UMTS networks in many countries were upgraded with High-Speed Downlink Packet Access (HSDPA), sometimes known as 3.5G. HSDPA enabled downlink transfer speeds of up to 21 Mbps. High-Speed Uplink Packet Access (HSUPA) was implemented for higher uplink transfer speed. In 2008, the 3GPP introduced a Long Term Evolution (LTE) technology to move from UMTS to 4G with speeds of 100 Mbps downlink and 50 Mbps uplink, using a next-generation air interface technology based upon orthogonal frequency-division multiplexing (OFDM).

The era form 2010 to date is known as fourth-generation (4G) mobile networking system and theoretically, the speeds are increased up to 1000 Mbps in downlink and 500 Mbps for uplink [24]. This technology is also called as LTE Advanced (LTE-A) in which mobile devices are used for many purposes.

Mobile network generations up to 4G continuously increased the data rates and reached up to 1000 Mbps [25]. Obviously, there will be a huge increase in terms of speed in 5G but there is focus on other factors as well. For example, many more devices can be connected to the same base station, data communication will be made more efficiently, coverage areas will be expanded, battery efficiency and durability will increase, and so on.

1.2. Motivation

The traditional homogeneous cellular communication system may not provide services to subscribers with good quality and performance in some scenarios, such as in dense urban areas, indoor environment, and cell edge areas, etc. The heterogeneous networks (HetNets) appear as a better solution for these challenges [26]. The HetNet is a system where the typical macrocell is incorporated by smallcells in those areas where the macrocell signals are weak or its coverage is poor. The deployment of smallcells inside the macrocell may improve the spectral efficiency and data rates of the system. By using HetNet technology, many benefits can be achieved; however, proper management of the radio resource needs to be addressed, otherwise, the risk of employing overlapping frequencies collision occurs which severely affects the system performance. The frequency collision occurs because of using the same frequency bands, which is known as co-channel interference (CCI) [27]. In Figure 1.1, two CCIs are explained such as co-tier interference and cross-tier interference. A co-tier interference occurs when a UE receives downlink signals from two or more same type of cells which is shown in Figure 1.1 (a). Contrary, a cross-tier interference occurs when a UE receives downlink signals from two or more than two different types of cells such as macrocell and femtocell which is demonstrated in Figure 1.1 (b). In order to reduce the effect of CCI and achieve higher spectral efficiency in LTE-A HetNet, a novel Radio Resource Management (RRM) is proposed in this dissertation. We use a new Fractional Frequency Reuse with Three Sectors and Three Layers (FFR-3SL) method which split the entire macrocell into three sectors and three layers. Consequently, the available bandwidth is divided into seven subbands and shared among the Macro UEs (MUE) and Femto UEs (FUE) in their respective zones.

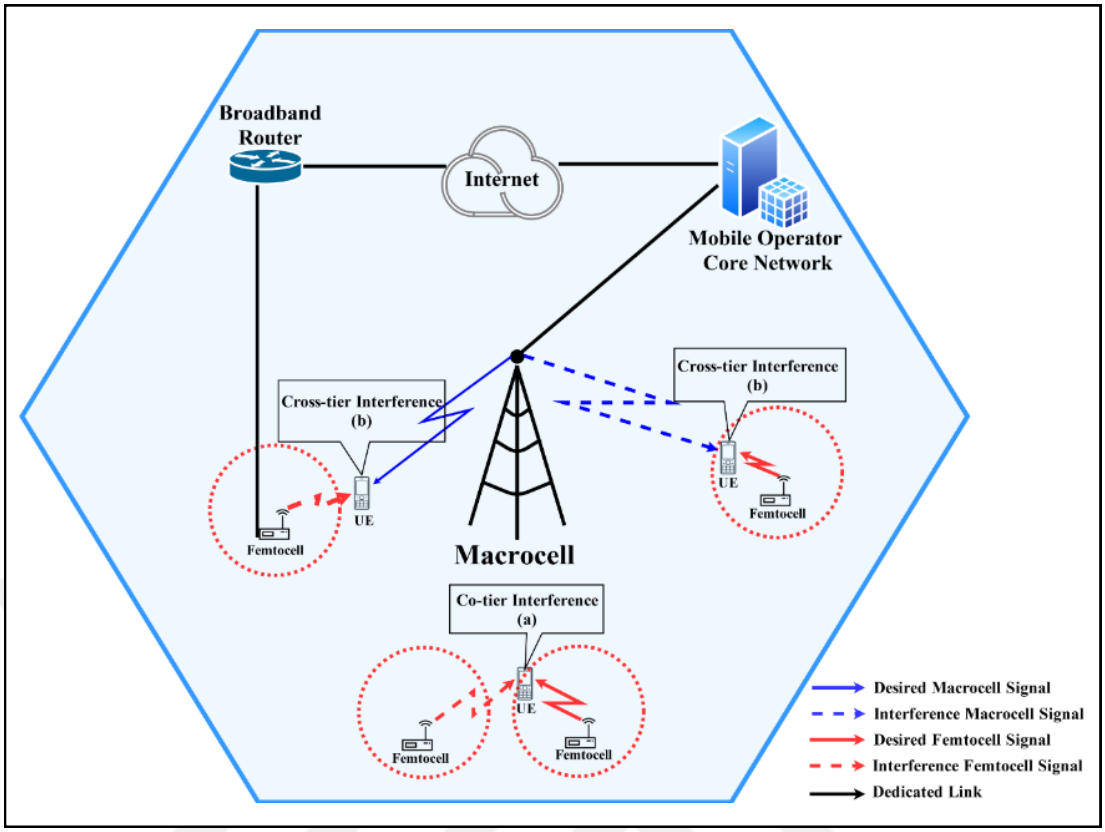

Figure 1.1. Co-channel interferences in LTE-A HetNet

1.3. Literature Review

Due to the sheer growth of mobile broadband subscriptions, the demand for a high data rate has increased. According to Ericsson mobility report [28], until 2021 the number of mobile broadband subscriptions will reach up to 9 billion, where 7.7 billion will use the mobile data [29]. Furthermore, the growth of smartphone data and video traffics will be multiplied 20 and 25 times respectively. The Cisco calculated that the mobile data is reached up to 11.2 Exabytes per month by 2017 and 50 Exabytes per month is expected until 2022 [30]. LTE-A is a promising technology that provides 300 Mbps download and 150 Mbps upload data speeds [31]. The present LTE-A system is based on a homogeneous network, where every single evolved Node-B (eNB) covers the whole cell and uses the same transmission power levels, modulation techniques, access schemes, antenna patterns to offer QoS to the User Equipment (UE) across the cell [32, 33]. On the contrary, such deployment reduces the coverage and capacity of the cell-edge users. The primary approach for solving the problem mentioned above is to shrink the cells, which will satisfy the increased demand for high data rates in cellular

systems and recover the signal to interference and noise ratio (SINR), but this approach is not economical and needs massive investments [4]. Therefore, the deployment of a heterogeneous network (HetNet) is more scalable and useful for both operators as well as users. It is expected that this approach will improve the system throughput and expand the coverage and enhance the capacity of a macrocell in a cost-effective manner [34].

On the other hand, nearly 90% of data services and two-thirds of calls are generated from inside the buildings, and the indoor users are complaining of poor coverage because of the walls and other obstacles that weaken the strength of signals. Thus, the short-range femtocells are being deployed to extend the coverage for indoor users, i.e., offices, shopping malls, and homes, etc. subscribers [26, 35]. The femtocell is also known as Home Evolved Node B (HeNBs), and the typical radius of a femtocell coverage area is around 30 m and the transmit power of a femtocell is usually less than 0.1 W ($\leq$ 20dBm) [36].

Figure 1.2 describes how HeNBs are connected to Evolved Packet Core (EPC) with Asynchronous Digital Subscribers Line (ADSL) link. This type of architecture is usually known as the HetNet [37, 38]. The HeNBs are connected with the HeNB Gateway, and then HeNB Gateway is linked with EPC of the core system [39]. The eNBs are directly connected with each other through x2 links. S1 is a link between eNB and Mobility Management Entity and Serving Gateways (MME/SGW). In HetNet the eNBs and HeNBs generally use the same frequency band to obtain the required cell splitting gain [40]. As a result, the HetNet provides better coverage and higher throughput as compared to conventional network. However, to successfully install the femtocell architecture, different challenges need to be considered. Among other problems in LTE-A HetNets, the main difficulty is to manage the interference because femtocells and macrocells operate on the same frequency which causes a cross-tier interference, while femtocell generate a co-tier interference with nearby femtocells [41].

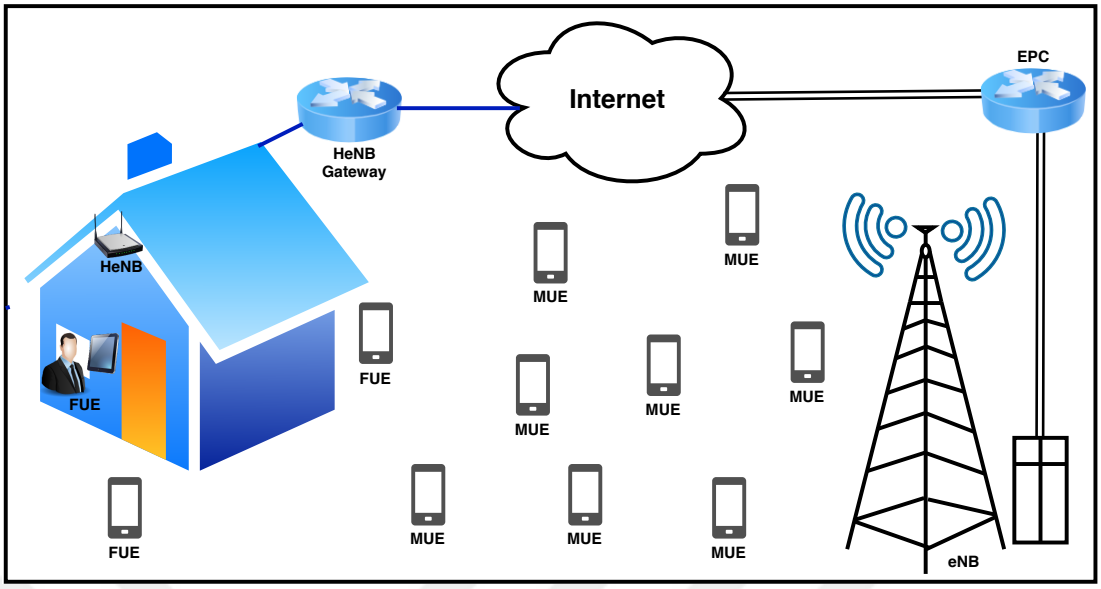

Figure 1.2. An LTE-A HetNet architecture

There are many solutions proposed in the literature; however, the most effective solution is the Fractional Frequency Reuse (FFR) technique which can reduce the CCI in LTE-A HetNets expeditiously [42, 43]. The authors in [44] investigated the FFR and non-FFR approaches and expressed that the FFR scheme performs much better than non-FFR in terms of throughput and capacity. Some of the authors implemented different FFR techniques in their studies [45–51]. The authors in [52] presented an Optimal Static FFR (OSFFR) scheme for two-tier HetNets in LTE-Advanced systems in order to increase throughput in macrocell edge UEs and made a comparison among four different FFR schemes, i.e., strict FFR, soft FFR, FFR-3, and OSFFR schemes. According to their simulation results, the OSFFR scheme outperforms than the other three state-of-the-art FFR schemes. Nevertheless, the subband distribution among femtocells is not addressed, therefore, co-tier interference may occur among femtocells. In [53], a resource allocation scheme by using FFR with three regions (FFR-3R) is proposed for LTE-A Orthogonal Frequency Division Multiple Access (OFDMA) based HetNet. The simulation results show an improvement in macrocells throughput because of the decline in cross-tier interference, however, the effect of co-tier interference remains the same. A similar study is presented in [54, 55] where the authors employ the same FFR scheme with three sectors (FFR-3) to overcome the effect of CCI in HetNet. The cross-tier interference is reduced and edge layer UEs achieve higher throughput. The co-tier interference among femtocells is not addressed properly.

1.4. Scope of the Thesis

The main objective of this thesis is to investigate the feasibility of applying new FFR for mitigating the interference issues and to allocate the radio resources efficiently in LTE-A HetNet in order to achieve better system performance.

1. A new approach called as fractional frequency reuse with three sectors and three layers (FFR-3SL) is introduced in which the whole macrocell coverage area is segmented into three sectors and three layers and become nice zones in a typical macrocell region. To cover these zones, the available bandwidth is divided into seven small fractions of subbands which referred to radio resources as well.

2. In order to improve the throughput of the LTE-A HetNet system, a user location distribution based fractional frequency reuse strategy is implemented and analyze the performance of the system.

3. A Transmit Power Control (TPC) algorithm is proposed to reduce the cross-tier interference caused by the femtocells when deploying inside the macrocells.

2. LTE-A HETEROGENEOUS NETWORKS (HETNETS)

2.1. Introduction

The third generation partnership project (3GPP) is responsible to set up the standards for wireless communication systems [56]. The goal is to establish infrastructures for the installation of seven trillion wireless devices used by seven billion people in the world population [57]. In 2008, the 3GPP introduced the first state of the art technology in its Release-8, which gained a lot of attention [58]. This technology is as known as long term evolution (LTE) technology that enabled the whole vendors under the one umbrella. Just after two years, 3GPP announced a long term evolution advanced (LTE-A) with some extra features in its Release-12 [59]. In this chapter, we discuss LTE, LTE-A, and their features which enabled the telecommunication more diverse.

2.2. Long Term Evolution (LTE)

Long Term Evolution (LTE) relates to the standards set up for a smooth and efficient transition toward more advanced leading-edge technologies to increase the capacity and speed of wireless communication systems [60]. LTE provides high speed wireless broadband to its subscribers. The common LTE features include IP based extended networks, ensures the quality of service (QoS) between end-users, high downloading speed of about 100 Mbps in downlink and about 50 Mbps in uplink, expand the macrocell capacity and can handle more 100 active users on the same times, and support fast mobility [61].

LTE is considered as 3.5G network and beyond that, with the capacity to support the high demand for connectivity from new consumer devices tailored to new mobile applications [62]. In an LTE live air demo, web browsing, HD video, and telecommunications are demonstrated simultaneously inside a single computer moving within a vehicle at 108 kilometers per hour [63].

The main features of LTE are as follows:

1. Orthogonal frequency division multiplexing (OFDM) and multiple input multiple output (MIMO) are used as radio access and advanced antenna, respectively.

2. System architecture evolution (SAE) is used as a new network architecture.

2.2.1. OFDM and OFDMA

The entire LTE and LTE-A networks are internet protocol (IP) based which are capable of transferring voice, video and data traffic in a reliable and secure way [64]. The core principle behind using IP is to assign dynamic addresses to the subscribers when a mobile switches on and to release when it switches off [65]. Moreover, orthogonal frequency division multiplexing (OFDM) is a revolutionary radical communication technology, which essentially forms the bases for all 4G wireless communication systems [66]. In other words, all the fourth and fifth generation technologies are based on OFDM. It is a key technology for future generation wireless communication systems.

IEEE 802.16 WiMAX and 3GPP LTE-Advanced technologies are purely OFDM based technologies. These technologies provide Wireless Broadband services with several advantages to the end-users [67]. OFDM based technologies claim of more 100 Mbps as uplink and downlink data rates. LTE uses orthogonal frequency division multiple access (OFDMA) for downlink as an access method. Due to the complex calculation in OFDMA, single carrier frequency division multiple access (SC-FDM) is used as an access method for uplink [68]. To achieve high data rates, the resources are shared among many active users in OFDMA, on the other hand, the SC-FDMA uses a single subcarrier for each UE [69]. The stages of LTE signal generation are given in the Figure 2.1.

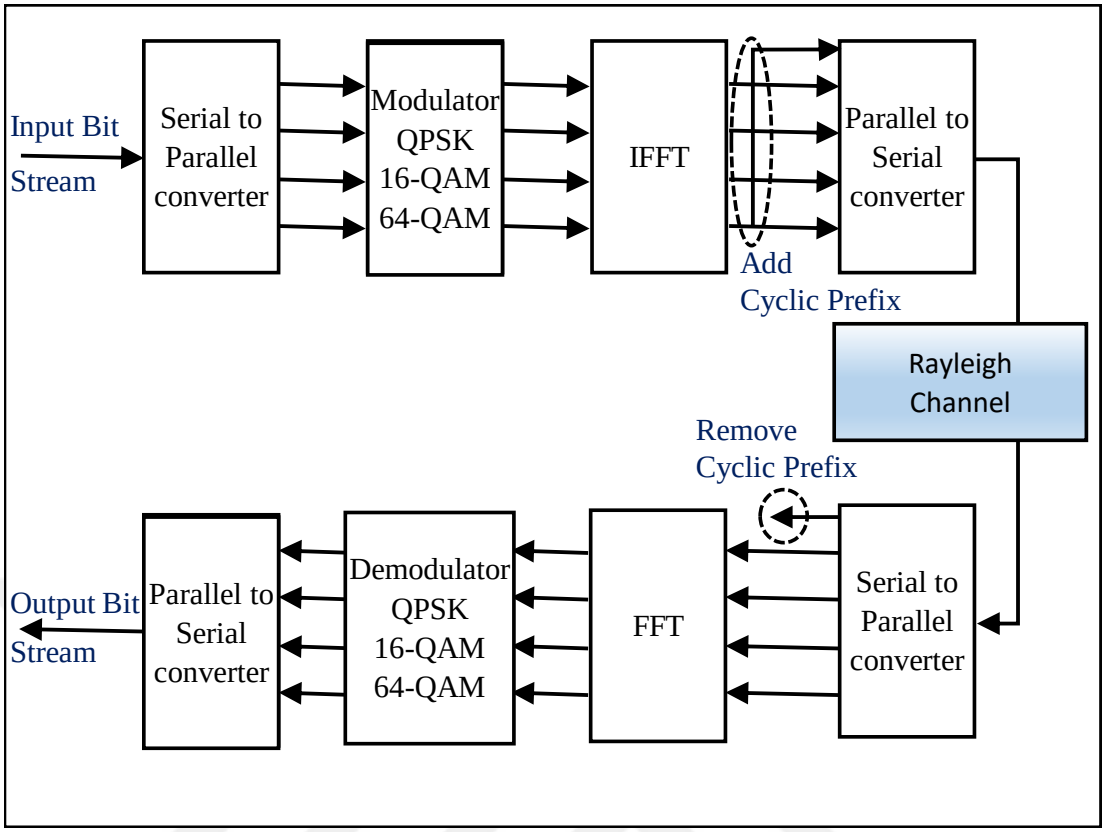

Figure 2.1. Data flow of LTE-A OFDM signal

OFDM Signal:

The Orthogonal Frequency Division Multiplexing (OFDM) signal for LTE downlink data transmission given in Figure 2.1. The input data stream is transmitted in Orthogonal Frequency Division Multiple Access (OFDMA) over parallel subcarriers of 15 kHz each. The subcarriers are further divided into symbols and carried by Resource Element (RE). Each RE consists of 66.7 μs of duration in time domain and one subcarrier of 15 kHz in the frequency domain. In order to transmit these RE, first the data is modulated with specific modulation scheme. There are three different modulation schemes such as QPSK, 16-QAM, and 64 QAM used in LTE. The modulation scheme is depends on the physical channel mapped on the resource grid. Suppose, we gave 8 bits of data to be transmitted using QPSK modulation. The data will be divided into four parallel streams of two bits, phase and amplitude representation is done according to the QPSK constellation. Finally, data is placed over the RE by adjusting the phase and amplitude of subcarrier to those derived for the data stream.

Mathematically, it means multiplying the complex modulation symbol to the corresponding subcarrier frequency. Thus, in a 20 MHz channel, all the 1200 RE caring 1200 symbols over 1200 subcarriers are modulated with the appropriate modulation scheme. Now, since the data is modulated over 1200 subcarriers, A transmitter will require 1200 oscillators for its generation, and 1200 will be required by the receiver for proper demodulation. The hardware complexity and sheer amount of power consumption would have left OFDM to theoretical idea and far from implementation. OFDM was made reality with the advent of Digital Signal Processing (DSP) techniques. So, instead of using 1200 oscillators Inverse Fast Fourier Transform (IFFT) solves this problem by converting the parallel frequency domain signals into samples of a composite time domain signal which are much easier to generate at the transmitter side. As the data is sampled by IFFT, samples must be taken above the Nyquist rate faithful reproduction at the receiver. The Inverse Fast Fourier Transform (IFFT) is used to convert the parallel frequency domain signals into sample of a composite time domain signal. The LTE-A supports many frequency bandwidths which have different number of Resource Blocks (RB) presented in Table 2.1.

Table 2.1. The number of Resource Blocks (RB) supported by LTE-A

Total Bandwidth	**Guard Band**	**Available Band**	**Resource Blocks (RBs)**
1.4 MHz	2 x 0.16 MHz	1.08 MHz	6
3 MHz	2 x 0.15 MHz	2.7 MHz	15
5 MHz	2 x 0.25 MHz	4.5 MHz	25
10 MHz	2 x 0.5 MHz	9 MHz	50
15 MHz	2 x 0.75 MHz	13.5 MHz	75
20 MHz	2 x 1 MHz	18 MHz	100

The OFDM signal is given by,

$$S_i(t) = x_i e^{j2\pi f_i t} \tag{2.1}$$

Here f_i is the center frequency of i^{th} subcarrier, while x_i is the data transmitted on the i^{th} subcarrier.

$$S(t) = \sum_{i=1}^{N} x_i e^{j2\pi f_i \frac{B}{N} t} \tag{2.2}$$

Cyclic Prefix:

One of the primary reasons for using OFDM as a modulation format within LTE-A is its resilience to multi path delays and spread. However it is still necessary to implement methods of adding resilience to the system. This helps overcome the inter-symbol interference (ISI) which occurs as a result of symbols time delay [70]. In the time domain, the ISI can be reduced by inserting a guard period into the timing at the beginning of each data symbol. It is then possible to copy a section from the end of the symbol to the beginning of that symbol [71]. This method called as the cyclic prefix (CP). The receiver can then sample the waveform at the optimum time and avoid any ISI caused by reflections that are delayed by times up to the length of the CP.

The length of the CP is important, if it is not long enough then it will not counteract the multi path reflection delay spread [72]. If it is too long, then it will reduce the data throughput capacity. For LTE, the standard length of the cyclic prefix has been chosen to be 4.69 μs. This enables the system to accommodate path variations of up to 1.4 km. With the symbol length in LTE set to 66.7 μs [73].

For OFDM systems the symbol length is equal to the reciprocal of the carrier spacing so the orthogonality is achieved. The length of one time slot with a carrier spacing of 15 kHz is equal to 500 μs, which include seven normal CPs $(5.20+6\times 4.69)$ μs and seven symbols of 66.7 μs each.

2.2.2. LTE System Architecture Evolution (SAE)

The LTE System Architecture Evolution (SAE) architecture and concepts have been designed for efficient support and usage of all IP -based services. The architecture is based on an evolution of the existing GSM/WCDMA core network, with simplified operations and smooth, cost-efficient deployment [74] as in Figure 2.2. Moreover, work was recently initiated between 3GPP and 3GPP2 (the CDMA standardization body) to optimize inter-working between CDMA and LTE–SAE. This means that CDMA operators will be able to evolve their networks to LTE SAE and enjoy the economies of scale and global chipset volumes that have been such strong benefits for GSM and WCDMA [75].

The main features of LTE SAE are: it reduces the cost per bit, increases service provisioning, provides flexible use of existing and new frequency bands, a simplified architecture and directly connected interfaces, and reasonable power consumption, etc.

2.3. Long Term Evolution Advanced (LTE-A)

In 2010, the 3GPP launched long term evolution advanced (LTE-A) as a 4G technology. As the name implies, LTE-A is just an enhanced version of LTE standards [76]. It uses a variety of additional techniques to warrant the "advanced" name. The new functionalities introduced in LTE-Advanced are Carrier Aggregation (CA), better use of existing MIMO, deployment of relay nodes and support for the heterogeneous network (HetNet) [77]. All of these are designed to increase the stability, bandwidth, and speed of LTE networks and connections.

2.4. LTE-A Heterogeneous Network (HetNet)

The increase in traffic demand is overloading cellular networks, forcing them to operate close to (and often beyond) their capacity limits. Upgrading to LTE or LTE-advanced, as well as the deployment of additional network infrastructure could help alleviate this capacity crunch [78], but reports already suggest that such solutions are bound to face the same problems [79]. Furthermore, these solutions may not be cost-effective from the operators' perspective: they imply an increased cost (for power, location rents, deployment, and maintenance) without a similar increase in revenues.

The typical mobile cellular communication systems use a homogeneous network architecture, where a network of macrocell base stations provides coverage to the user equipment (UEs) in each cell. In such a homogeneous network, the macrocells have similar transmission power levels, antenna patterns, access schemes, modulation technique, receiver noise floors, and back-haul connectivity to offer similar QoS to the UEs across all cells [80]. However, such a deployment especially degrades the coverage and capacity of the cell-edge users.

One of the approaches to solve this problem is to employ the concept of cell splitting. However, this approach may not be economically feasible since it involves deploying

more macrocells within the network and site acquisition for macrocells in dense urban areas becomes a difficult proposition for the operators [81]. Therefore, evolving LTE-A systems are adopting a more flexible and scalable approach using a hierarchical cell deployment model where smallcells are overlaid on the macrocells. The resulting network architecture is also referred to as a heterogeneous network (HetNet) architecture. Figure 2.2 demonstrate the LTE-A HetNet architecture, where evolved node base station (eNB) indicate macrocell while Home eNB (HeNB) means femtocell.

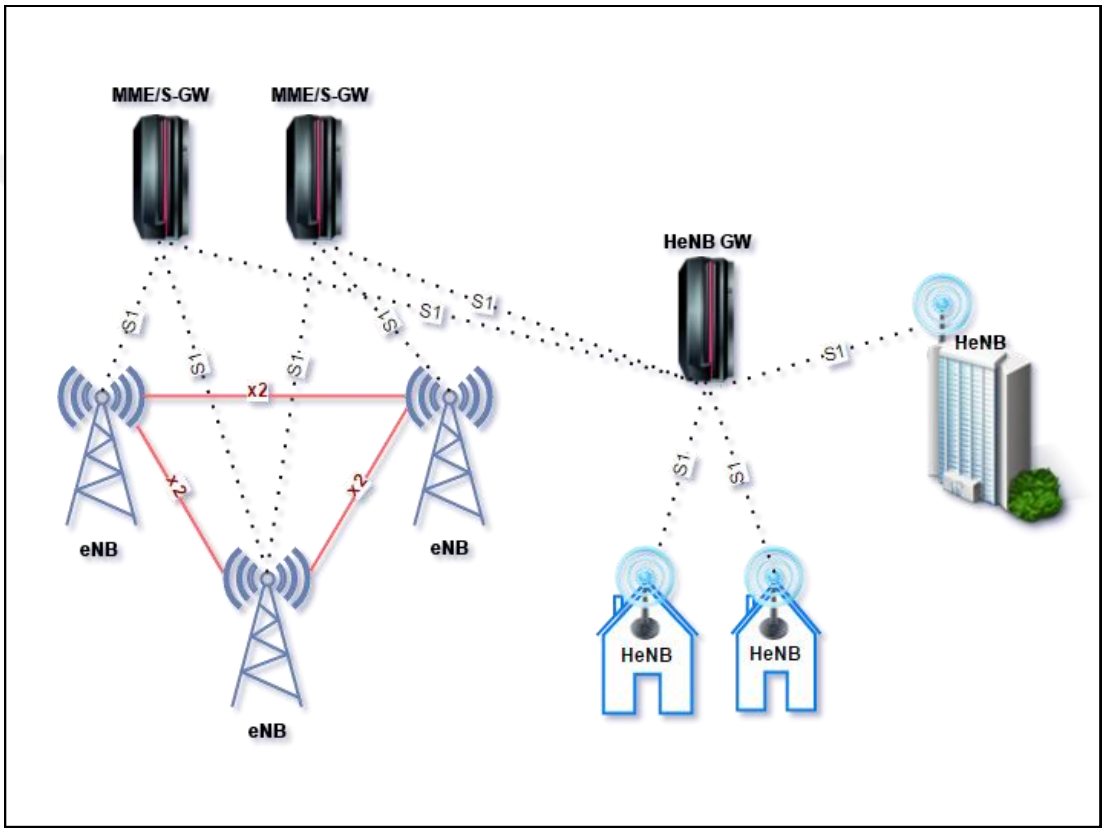

Figure 2.2. LTE-A heterogeneous network architecture

Such architecture is useful for both the operators and subscribers. Because this approach is expected not only to increase the coverage and capacity of the cell but also to improve the broadband user experience within the cell in a ubiquitous and cost-effective manner. In a HetNet, smallcells are envisioned as traffic off-loading spots in the radio access network (RAN) to decrease the congestion in macrocells and enhance the users' QoS experience [82].

2.4.1. Smallcells

Smallcells are plug and play devices that use the existing broadband connection and connect to the operator's core network. It provides short-range 10 to 30 m coverage and achieves high throughput and better capacity. Smallcells support wireless applications for homes and enterprises as well as metropolitan and rural public spaces. Due to the smaller coverage areas, the same licensed frequency band can be efficiently reused multiple times within the smallcells in a HetNet, thus improving the spectral efficiency per unit area the capacity of the network. There are many types of smallcells used in LTE-A HetNet such as femtocells, picocells, and microcells, etc. However, the femtocell is recognized as one of the promising technologies. Femtocells are sometimes referred to as HeNBs in LTE-A standards, which is a low power and easy to plug-in device which can be installed at homes, shopping malls and crowded places in urban areas [83]. It provides a short-range coverage to the indoor UEs. The main advantages of using HeNBs include low cost, IP back-hauling and frequency reuse, provide high capacity, Low battery usage, and seamless transition between wired and wireless connecting devices [84]. However, in order to deploy the LTE-A successfully, several challenges such as Co-Channel Interference (CCI) and Radio Resource Management (RRM) need to be addressed.

2.5. The Problem Statement in the Existing Network

When there are a huge number of femtocells deployed in a HetNet system, the macrocells and the femtocell have to share the same spectrum. Hence, the downlink and uplink CCI occur. Specifically, the downlink transmissions from the femtocell cause strong interference at a nearby macrocell's UE and may interrupt the received macrocell signal at the macrocell's UE, thereby degrading the performance and becoming intolerable. Hence, CCI is one of the major barriers for the successful coexistence of macrocells and femtocells in a HetNet. The solutions to solve the CCI issue are given in the proceeding Chapter. On top of these, in order to achieve high throughput and better efficiency, radio resources in a HetNet should be efficiently utilized in a well-organized manner.

3. FRACTIONAL FREQUENCY REUSE METHOD FOR RESOURCE MANAGEMENT IN LTE-A HETNETS

3.1. Introduction

The telecommunication industry progresses toward the development of the fifth generation (5G) standard that requires coexistence of heterogeneous networks (HetNets). The reason for using HetNets is to provide effective wireless coverage to mobile subscribers and other wireless appliances in both indoor and outdoor environments. In other words, the demand for wireless services at indoor environment continuously increases as the mobile subscribers grow [62]. It is foreseen that by the end of 2021, two-thirds of mobile subscribers will consume data in the indoor environment [30, 85]. Therefore, HetNet appears as an attractive solution for the envisioned 5G mobile cellular networking system. In specifications of the Long Term Evolution-Advanced (LTE-A) networks, a HetNet is a multi-tier network system, where different smallcells are deployed especially in crowded areas and cell-edges over the existing cellular networks [86]. Smallcells are short ranged, low powered, and easy to plug-in radio access nodes using licensed and unlicensed frequency bands [87]. The smallcells consist of relay nodes, microcells, picocells, and femtocells, which are deployed at different places according to user requirements. One of the significant smallcells is femtocell, which can be located at homes, offices, and public places to provide coverage to the indoor subscribers. According to the Third Generation Partnership Project (3GPP) Release-12, a femtocell is also known as Home Evolved Node Base-Station (HeNB) [88]. It covers relatively smaller areas, i.e., 20 to 30 meters and provides high data throughput to the User Equipment (UE). Thanks to femtocells, users who are at the edges and shadow areas of a macrocell region can also be served. Furthermore, 5G Internet of Things (IoT) systems may also employ femtocells in order to connect home appliances to the core network of the system [89].

In LTE-A HetNet system, macrocells and femtocells operates on the same frequency channel. As a result, Co-Channel Interference (CCI) occurs. There are two major types

of CCI, described in Figure 3.1, which may arise in different situations. When the CCI occurs among the same type of cells i.e., femtocell-femtocell, it is called co-tier interference, like scenario (A) has depicted in Figure 3.1. On the other hand, the CCI among different type of cells is called cross-tier interference, such as the scenario (B) as shown in Figure 3.1. Ultimately, interference degrades the quality of the signal and creates critical problems during wireless communication. Therefore, different methods are proposed in the literature to control CCI in HetNets. Dedicated channel link is the most straightforward technique to solve this issue; however, there is a high probability of wasting the radio resources [90]. Moreover, Carrier Aggregation (CA) and Enhanced Inter-Cell Interference Coordination (E-ICIC) methods are introduced in 3GPP Release-12 [91]. Besides that, researchers are still investigating different techniques and comparing them to find out the best solution. In [92], a Power Control Algorithm (PCA) and simulation tool are introduced to mitigate the co-tier interference among femtocells. In [93], L. Zhang et al. suggested a cognitive radio approach, where the neighboring femtocells exchange the path-loss information to each other and select the carriers aggregation to estimate the co-tier interference. The above two approaches consider only co-tier interferences but ignore the cross-tier interferences completely.

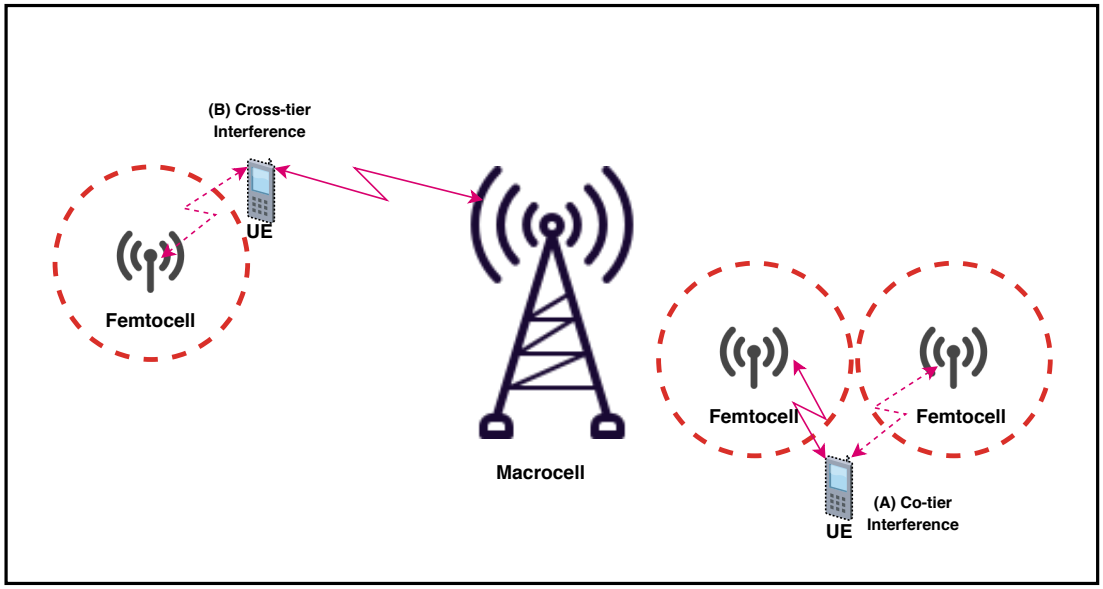

Figure 3.1. Different interference scenarios in LTE-A HetNet downlink channel

Fractional Frequency Reuse (FFR) as a resource allocation scheme is an effective technique used to reduce the CCI in LTE-A HetNets [42, 43]. The authors in [44] investigated the FFR and non-FFR approaches and expressed that FFR scheme performs

much better than non-FFR in terms of throughput and capacity. Consequently, many researchers studied different FFR schemes [45–51], and they come up with new ideas. The authors in [52], presented an Optimal Static FFR (OSFFR) scheme for two-tier HetNets in LTE-Advanced systems in order to increase throughput in macrocell edge UEs and made a comparison among four different FFR schemes, i.e., strict FFR, soft FFR, FFR-3, and OSFFR schemes. According to their simulation results, OSFFR scheme outperforms than the other three state-of-the-art FFR schemes. Nevertheless, the subband distribution among femtocells is not addressed, therefore, co-tier interference may occur among femtocells. N. Fradi et al. in [53], proposed a resource allocation scheme using FFR with three regions (FFR-3R) in LTE-A Orthogonal Frequency Division Multiple Access (OFDMA) based HetNet. The simulation results show an improvement in macrocells throughput because of the decline in cross-tier interference, however, the effect of co-tier interference remains the same. A similar study is presented in [54, 55], where the authors employ the same FFR scheme with three sectors (FFR-3) to overcome the effect of CCI in HetNet. The cross-tier interference is reduced and edge layer UEs achieve higher throughput. The co-tier interference among femtocells is not addressed properly.

In this study, a new FFR strategy is proposed for LTE-A HetNets, where the whole macrocell coverage area is segmented into three sectors and three layers. While on the other hand, the total radio frequency band is divided into seven frequency subbands (radio resources). The bigger chunk of the frequency band is shared among the central layer while the other subbands are distributed over the remaining zones of the middle and outer-most layers. Furthermore, the subbands are re-used by femtocells in other zones of the macrocell coverage area in a specific and well-organized manner. In order to implement our strategy, a novel FFR algorithm is proposed, which reduces not only CCI interferences but also tries to finds the most suitable subband for newly deployed femtocell when it switches on in any sector or zones of the macrocell region. A Monte Carlo simulation is performed to accurately assess the performance of our proposed method. Unlike the existing studies in literature, we focus on the central area because we assume that the central area is highly populated zones. The major contribution of this study is to propose a new FFR scheme such that it provides reduced co-tier and cross-tier

interferences, improved femto UEs (FUEs) and macro UEs (MUEs) throughput, better efficiency of the active UEs connection, and UE satisfaction for higher radio resources demand. The variables (symbols), which are used in this study are summarized in the Nomenclature.

One of the most favorable and reliable techniques to manage and control CCI in HetNets is FFR scheme, where the radio resources (subbands) are properly allocated among femtocells and macrocells. The basic idea behind the FFR technique is to divide the total bandwidth into several small subbands and then assign to different zones of the macrocell region. Furthermore, the same subbands are re-used by femtocells in other zones of the macrocells region, separated by considerable distance to avoid interference. However, the macrocell coverage area must be segmented in an organized manner, in order to reduce the effect of CCI. In this study, three most cited methods are considered and summarized in Table 3.1.

Table 3.1. Summary of existing popular FFR schemes

Technique	**Layers**	**Sectors**	**Zones**	**SBs**
OSFFR [52]	2	6	12	7
FFR-3R [53]	3	3	9	4
FFR-3 [54]	2	3	6	4
FFR-3SL (Proposed)	3	3	9	7

3.2. Existing FFR Methods

3.2.1. OSFFR

The OSFFR scheme is proposed by N. Saqueb et al. in [52], where the macrocell coverage area is split into two layers and six sectors. As a result, the macrocell is segmented into twelve total zones, on the other hand, the total available bandwidth is

divided into seven subbands. The first (SB) is shared among all the zones of the central layer, while the remaining subbands are distributed among the six zones of edge layer of the macrocell region. In addition, all the subbands are re-used by femtocells in different zones of the macrocell coverage area in such a way to avoid the cross-tier interference. This scheme improves the performance of the system and reduces cross-tier interference, nevertheless, co-tier interference is not rectified properly. Moreover, the effect of (MBS) transmit power among narrow sectors is quite difficult to manage in this scheme.

3.2.2. FFR-3R

Another FFR strategy with three regions (FFR-3R) is presented in [53] by Fradi and others, where the entire macrocell coverage area is separated into three layers, named as inner, intermediate and outer regions. Alongside, the macrocell coverage area is further split into three sectors. In order to fulfill the nine zones, the total available bandwidth is divided into four (A, B, C, D) subbands. The subband A is shared among all the center zones, while other subbands (B, C, D) are shared among different zones of intermediate and outer regions. Furthermore, all the subbands are re-used by femtocells in different zones of the macrocell coverage areas. In this scheme, the allotment of subbands is not configured efficiently. As a result, higher chances of CCI may occur among MUEs and FUEs due to frequency re-use factor.

3.2.3. FFR-3

P. Lee et al. suggested an idea in [54] by using the FFR method along with three sectors (FFR-3) and two layers. In this method, the overall macrocell coverage area is separated into central and edge layers. Likewise, each layer is then split into three sectors. As a result, the macrocell is segmented into six total zones. Contrarily, the total available bandwidth is divided into four subbands. The first subband is thoroughly shared among all the zones of the central layer, while the other three subbands are distributed among edge layer's zones of the macrocell region. Additionally, all the subbands are re-used by femtocells in other zones of the macrocell region. This strategy is very useful to avoid cross-tier interference, however, there is no proper mechanism explained to mitigate the co-tier interferences when it happens.

3.3. System Model

Our new method referred to as Fractional Frequency Re-use with Three Sectors, and Three Layer (FFR-3SL) which is published in [94] is considered in this study. The principle idea of the proposed method is to divide the total allocated frequency band into smaller fractions (subbands), which are then distributed among femtocells and the macrocell in different areas of the coverage region. The detailed network topology and a viable algorithm of the proposed method are discussed below.

The proposed network topology is demonstrated in Figure 3.2, where the total frequency band is divided into seven subbands such as A, B, C, D, E, F and G. Furthermore, the whole macrocell coverage area is partitioned into three sectors, named as sector α, sector β, and sector γ, which are further segmented into three layers, named as central layer X, middle layer Y, and outer layer Z. For simplicity, we call the central layer as X_1, X_2, and X_3, middle layer as Y_1, Y_2, and Y_3 and the outer-most layer as Z_1, Z_2, and Z_3 zones. According to the proposed model, the subband G is solely reserved for MUEs available in the central layer. However, the subband G is not assigned to femtocells to re-use for FUEs in the other zones of the macrocell coverage region, because it is assumed that the number of MUEs is largely available in the central layer and quite close to MBS, and they should be given priority to use dedicated subband G. On the other hand, the subbands A, B, C, D, E, and F are reserved for MUEs in zones Y_i and Z_i ($i\varepsilon\{1,2,3\}$), respectively. After setting the subbands assignment for MUEs in macrocell regions, all the subbands except subband G are re-used by femtocells located in the other zones of the macrocell coverage area. Considering subband allocation among femtocells appropriately, groups of available subbands are defined for every sector. When a new femtocell is switched on, the system identifies its location by checking the reference signal received power (RSRP) values received from MBS, where RSRP is the predefined frequency measurement affix in reference signal [95]. Once, it identifies its location, then the most suitable subband is assigned to the i^{th} femtocell from the relevant group of subbands. An OFDMA based LTE-A HetNet system is used to investigate and compare the proposed method against the current methods. In LTE-A network system, the smallest unit to be allocated to every UE in the frequency domain of the downlink

channel is the resource block (RB), where each RB consists of 12 subcarriers. In term of the femtocell, an open access policy is adopted to utilize all the resources efficiently.

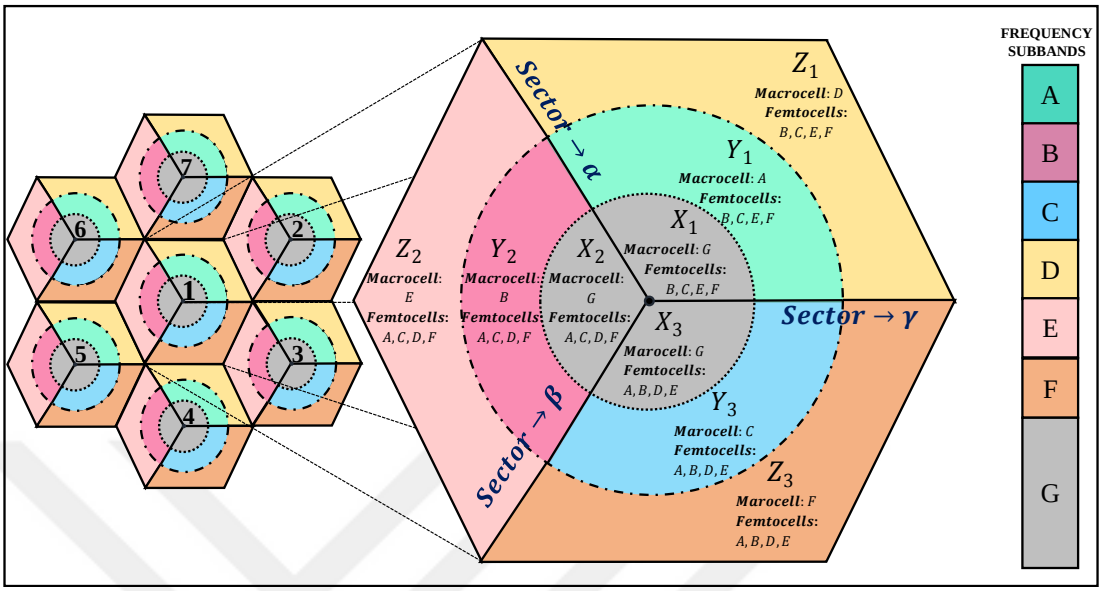

Figure 3.2. A HetNet topology of the proposed system model

3.3.1. Channel model

In the proposed model, a downlink wireless propagation model is considered, which comprises of path-loss (PL), log-normal shadowing and small scale fading between the Base Station (BS) and the UE. The UEs are randomly distributed with a uniform distribution over the macrocell coverage region. Besides, a single wall penetration loss is considered from indoor to outdoor transmission and vice-versa, while double wall penetration loss is considered among indoor to indoor transmissions.

Path-loss model:

The indoor PL model is defined in 3GPP Release-13 for LTE-A HetNet system [96] as given by,

$$\mathrm{PL(dB)} = 38.5 + 30\log_{10}(\mathrm{d}) + \mathrm{n} \tag{3.1}$$

where, term d is the distance between transmitter and receiver (in meters), while n is the wall penetration loss factor, if the distance is smaller than or equal to 10 meters, n is 7 dB, if the distance is greater than 10 meters and smaller than or equal to 20 meters, n is 10 dB. However, if the distance is greater than 20 meters, then n is 15 dB. The values

of n is given by,

$$n = \begin{cases} 7\text{dB} & d \leq 10\text{m} \\ 10\text{dB} & 10\text{m} \leq d \leq 20\text{m} \\ 15\text{dB} & d > 20\text{m} \end{cases} \tag{3.2}$$

Channel gain:

We consider a Rayleigh fading channel, in which the channel gain is defined as [97],

$$G = |h|^2.10^{(-PL+X_\sigma)/10} \tag{3.3}$$

where PL denotes path-loss in dB and X_σ is the shadowing effect of normal (Gaussian) distribution. h is a circularly symmetric complex Gaussian random variable with zero-mean and unit variance. So, |h| is Rayleigh distributed.

3.4. The Proposed Algorithm: FFR-3SL

In order to implement our new RRM strategy, we proposed a new algorithm so called FFR-3SL, which is given in Figure 3.3. The algorithm performs two primary functions. Firstly, it finds the total number of subbands and allocates them to appropriate zones in the macrocell coverage area. Secondly, it involves in selecting the most suitable subband for the femtocell deployed inside the coverage area of a macrocell. The second function avoids the chances of co-tier interference before it happens.

Algorithm 1: Radio resources (Subbands) allocation algorithm

```
// Subbands Assignment to Macrocell Regions
// Initialization
ω ← RBs;   // total available resource blocks (RBs)
K ← Subbands;   // total number of subbands
S ← Sectors;   // total number of sectors, S < K
L ← Layers;   // total number of layers, L < K
SB(K) ← Equation 3.3;   // central subband
SB(n) ← Equation 3.4;   // rest of the subbands
// Allotment of subbands to each layer's zone and group them in sectors
for n = 1 : S do
    X_n = SB(K);   // subbands for central layer
    Y_n = SB(n);   // subbands for middle layer
    Z_n = SB(n+S);   // subbands for outer layer
    Ω_n = [SB(n), SB(n+S), SB(K)];   // group of subbands for each
     sector e.g., [α, β, γ]
end
// Obtain the length of radius for central, middle, and outer layers
P_tx ← Input;   // set-up max. transmit power (dB) for central,
 middle and outer layers
ϒ_rx ← Input;   // set-up min. detectable RSRP (dB) received at
 the edge of each layer (Receiver Sensitivity)
d(m) = PLcalculation(P_tx, ϒ_rx);   // calculate the max radius for
 each layer by using the path-loss function
// Finding the best available subband for every femtocell (F)
for i = 1 : All femtocells (N_Fc) do
    F_i ← Initialize;
    φ_i^M;   // received signal frequencies at i^th femtocell (F_i)
     from macrocells (M), (we assume that cell IDs are
     inserted in the transmitted signal of macrocells)
    for j = 1 : S do
        if φ_i^M IN Ω_j then
            λ_i = SB \ Ω_j;   // subtract group of SBs used by
             macrocell (M) in that sector and get a group of
             available SBs for F_i
        end
        // Checking for nearby femtocells
        for j = 1 : All the femtocells (N_Fc) in a sector  if (j ≠ i) do
            ζ_{i,j}^F;   // received signals at F_i from femtocells of
             other sectors
            φ_{i,j}^F;   // Group of frequencies received at F_i from
             other femtocells of the same sector
            if φ_{i,j}^F IN λ_i then
                if j ≤ K − S then
                    for m = 1 : K − L do
                        φ_i^assigned = λ_i(m);
                    end
                else
                    l = arg[max(PL(d_{i,j}^F))]
                    φ_i^assigned = φ_{i,j}^F
                end
            end
        end
    end
end
```

Figure 3.3. Pseudo code of a proposed FFR-3SL algorithm

3.4.1. Subbands assignment to macrocell regions

The algorithm initially requires predefined parameters, where it takes total available RBs (ω), the total number of subbands (K), number of sectors per cell (S) and number of layers per cell (L). The number of RBs which are to be assigned for MUEs in the central zones is calculated as [52],

$$\mathrm{SB}(K) = \omega\left(\frac{\mathrm{r_c}}{\mathrm{R}}\right), \tag{3.4}$$

and the remaining RBs for MUEs and FUEs in the middle and outer layers are calculated as,

$$\mathrm{SB(n)} = \frac{[\omega - \mathrm{SB}(K)]}{K-1}, \qquad \mathrm{n} = 1,2,3,...,K-1 \tag{3.5}$$

where ω is total available RBs, $\mathrm{r_c}$ is the macrocell central layer radius and R is the macrocell radius as depicted in Figure 3.4. K is the total number of subbands.

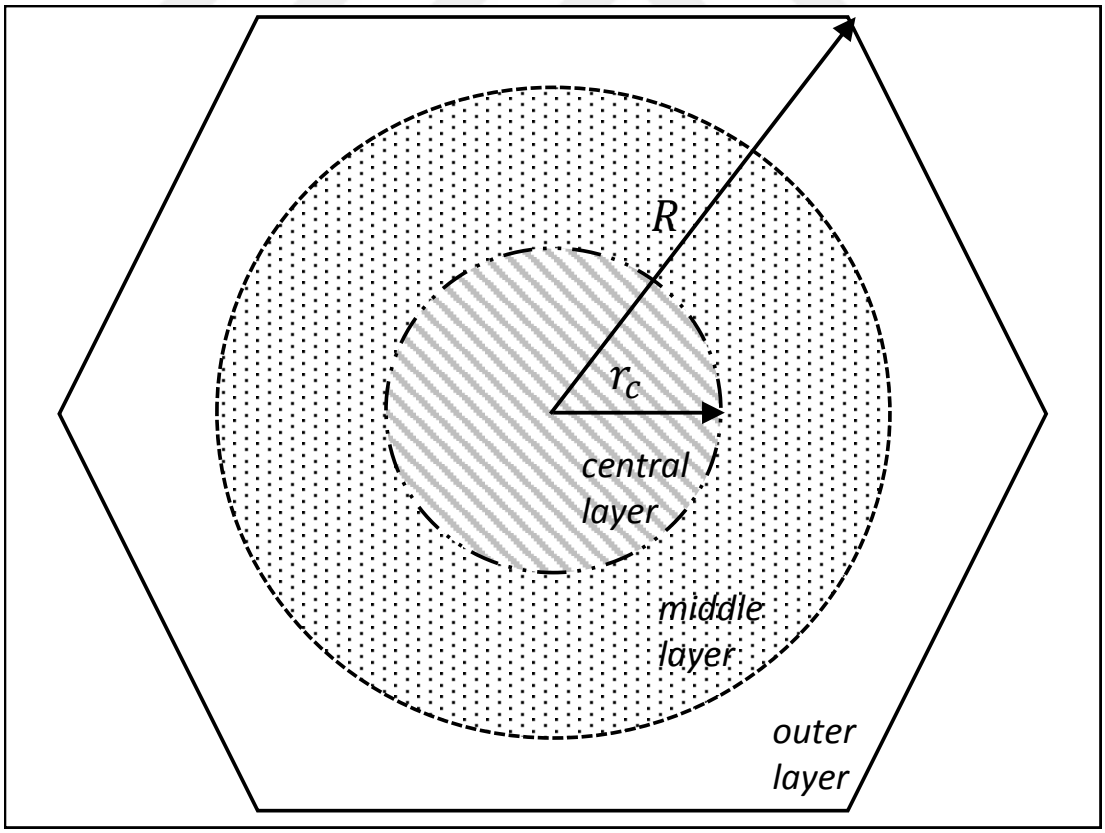

Figure 3.4. A ratio of central layer radius ($\mathrm{r_c}$) vs cell radius (R)

Example: In LTE-A network, each RB consists of 12 subcarriers and each subcarrier occupies 15 KHz. In other words, one RB occupies $12 \times 15 = 180$ KHz. Assume, if the system has 20 MHz bandwidth, 2 MHz is used for guard-band, while 18 MHz bandwidth is used for communication. The total number of RBs is, 18 MHz/180 KHz = 100 RBs.

Now, as stated in the network topology in Figure 3.2, we divide the total available bandwidth into seven subbands, and if the ratio of center radius to radius of macrocell $r_c/R = 0.4$, then the total number of RBs for seventh subband G used in the central layer zones is obtained by using (3.4), SB(7) is equal to 40 RBs.

In the same way, we can obtain the number of RBs for the remaining six subbands (A, B, C, D, E, F) which are utilized in middle and outer layers' zones of the macrocell coverage area by using (3.5); as a result, SB(1 TO 6) equals to 10 RBs per each SB. According to the above assumptions, all the SBs are allocated to the respective zones in each layer. Once all the SBs are distributed among macrocell regions, the SBs are grouped according to their relevant sectors.

3.4.2. Subband assignment for femtocells

The second step of the proposed algorithm is essential in order to search for the best available subband for all new femtocells when it connects to the core network. When a femtocell (F_i) is switched on, it registers to the system database. Once the registration is completed, it receives the RSRP values from the MBS and stores them in φ_i^M. On the basis of RSRP values, the system declares approximate location of F_i and its sector. In the next step, the λ sets a group of available subbands and discards the subbands used by macrocell in that sector. Every sector has a group of $\left(K \setminus S\right)$ usable subbands, where K denotes the total number of SBs, S is the number of sectors. Here, '\' indicates exclusion in set theory. Once, the group of available subbands is identified, the algorithm checks all the frequencies received from other femtocells nearby to avoid the co-tier interference. All the RSRP values received at F_i from other femtocells of the same sector are stored in $\varphi_{i,j}^F$, while the RSRP values received from femtocells of other sectors are discarded.

On a "first come first served" basis, the first subband from the group of usable subbands λ is assigned to the first active femtocell (F_i) and the second subband to the second active femtocell (F_{i+1}) and so on. Once all the available subbands in the group are assigned to femtocells, in the next step, the RSRP values stored in $\varphi^{F}_{i,j}$ are checked and the subband having the lowest RSRP value is selected an assigned frequency.

For example, if there are four SBs i.e., B, C, E, and F available for femtocell (F_i) in sector α, by using the proposed algorithm, the first, second, third and fourth deployed femtocells will get subband B, C, E, and F, respectively. Subsequently, when the fifth femtocell turns on in sector α, it searches for available subbands in that particular sector, however it returns with unavailable subband. Afterwards, it checks for the lowest received RSRP values, which are stored in $\varphi^{F}_{i,j}$. As a result, the farthest subband from this sector wise grouped in λ is assigned to the fifth requesting femtocell. Hence, femtocells have less chances to interfere with each other.

3.5. Performance Evaluation

We evaluate the performance of our proposed FFR-3SL method using some metrics which are explained below,

3.5.1. SINR

In LTE-A HetNets, the unwanted singles are also received from undesired transmitters in the downlink channel. The downlink SINR value received at UE in LTE-A networks heavily degrades due to the effect of interference that occurs among femtocells and macrocells. For MUE m using subcarrier k in macrocell M, its SINR is calculated by [98],

$$\mathrm{SINR}^{k}_{m} = \frac{P^{k}_{M} G^{k}_{m,M}}{N_o \Delta f + \sum_{m} P^{k}_{M'} G^{k}_{m,M'} + \sum_{m} P^{k}_{F} G^{k}_{m,F}} \tag{3.6}$$

where P^{k}_{M} and $G^{k}_{m,M}$ denote the transmit power of the macrocell M at subcarrier k and the channel gain of a MUE m from the desired macrocell M at subcarrier k, respectively. N_o is the white noise power density of the subcarrier spacing Δf, which is 15 KHz in LTE-A. $P^{k}_{M'}$ and $G^{k}_{m,M'}$ are the transmit power and channel gain at subcarrier k of a

MUE m from the interferer macrocells M′. While, the P_F^k and $G_{m,F}^k$ are transmit power and channel gain at subcarrier k of a MUE m from the interferer femtocells F.
Similarly, we obtain the SINR value from femtocell F at subcarrier k of a FUE f, the equation is described as,

$$SINR_f^k = \frac{P_F^k G_{f,F}^k}{N_o \Delta f + \sum_f P_{F'}^k G_{f,F'}^k + \sum_f P_M^k G_{f,M}^k} \tag{3.7}$$

where P_F^k and $G_{f,F}^k$ indicate the transmit power and the channel gain from the desired femtocell F at subcarrier k of a FUE f, respectively. The $P_{F'}^k$ and $G_{f,F'}^k$ are the transmit power and channel gain at subcarrier k of a FUE f from the undesired femtocell F′. Similarly, the P_M^k and $G_{m,M}^k$ are transmit power and channel gain respectively at subcarrier k of a FUE f from the macrocell M.

3.5.2. Channel capacity

The Shannon capacity of the system depends on SINR and system bandwidth, and for macrocell M at subcarrier k, it is calculated by,

$$C_m^k = \Delta f \log_2(1 + \alpha SINR_m^k), \tag{3.8}$$

where, $SINR_m^k$ is the SINR (dB) value of MUE m at subcarrier k, and $\alpha = -1.5/\ln(5BER)$. BER denotes the target bit error rate (10^{-6}).

The channel capacity for femtocell (F) is obtained by the following equation,

$$C_f^k = \Delta f \log_2(1 + \alpha SINR_f^k), \tag{3.9}$$

where $SINR_f^k$ is the SINR value of FUE f at subcarrier k.

3.5.3. Throughput

The throughput T_X, $X \varepsilon \{M, F\}$ achieved by macrocell M and femtocell F can be written as,

$$T_X = \sum_x \sum_k \psi_x^k C_x^k, \qquad X \varepsilon \{M, F\}, \quad x \varepsilon \{m, f\}. \tag{3.10}$$

where ψ_x^k indicates the subcarrier k assignment to UE x. When $\psi_x^k = 1$, it indicates that the subcarrier k is assigned to UE x, otherwise, $\psi_x^k = 0$.

Total throughput of the system is obtained by summing up the throughputs achieved by femtocells F and macrocells M,

$$T_{total} = T_M + T_F. \tag{3.11}$$

3.5.4. System efficiency

We defined system efficiency (η) is a ratio between number of UEs requested ($N_{UE,r}$) and number of UEs served ($N_{UE,s}$) and is given by,

$$\eta = \frac{N_{UE,s}}{N_{UE,r}} \times 100 \quad (\%). \tag{3.12}$$

3.5.5. User satisfaction

In wireless communication system, the SINR is used to examine the signal quality with respect to interference and noise. The higher SINR value means a better signal quality and UE satisfaction is defined as the probability of obtaining SINR value above or equal the threshold [99],

$$p(\Gamma_{thr}) = p(SINR_{UEs} \geq \Gamma_{thr}) = 1 - F(\Gamma_{thr}) \tag{3.13}$$

where F(.) and Γ_{thr} denote Cumulative Distribution Function (CDF) and SINR threshold value.

3.6. Simulation Setup and Parameters

Simulations are performed to assess the effectiveness of the proposed method in terms of previously defined performance measures. Our proposed method, FFR-3SL is also compared with the existing methods, FFR-3, OSFFR, and FFR-3R. Table 3.2 summarizes the simulation parameters. The two-tiered HetNet is considered with 7 macrocells and total 140 of femtocells. It is assumed that the femtocells are uniformly deployed within a macrocell region. Moreover, each macrocell consists of 100 UEs, which are also uniformly distributed over the macrocell coverage area. Besides, we

Table 3.2. Simulation parameters and values

Parameters	**Values**
Channel Bandwidth	20 MHz
Carrier Frequency	2.0 GHz
Sub-carrier spacing (Δf)	15 KHz
Total number of RBs	100
Macro-cell Radius	500 m
Femto-cell Radius	30 m
Total no. of macro–cell	7
Total no. of Femto-cells	140
No. of Femto-cells per Macro-cell	20
Max. no. of UEs per Femto-cells	5
Number of UEs per macro-cell	100
Macro-cell Transmit Powers	[20 , 15 , 10] Watt
Femto-cell Transmit Power	20 mWatt
White Noise Power Density	-174 dBm/Hz
Target BER	10^{-6}

applied the Round Robin scheduling algorithm and assigned random RBs to users varying from 2 to 10 RBs per UE to satisfy user higher radio resources demand. After setting network parameters, Monte Carlo simulations are performed, by running simulations 100 times. For each simulation run, number of femtocell deployed within macrocell region is increased linearly. The same procedure is executed for other existing FFR methods as well, with the same simulation conditions as in our method.

3.6.1. Results

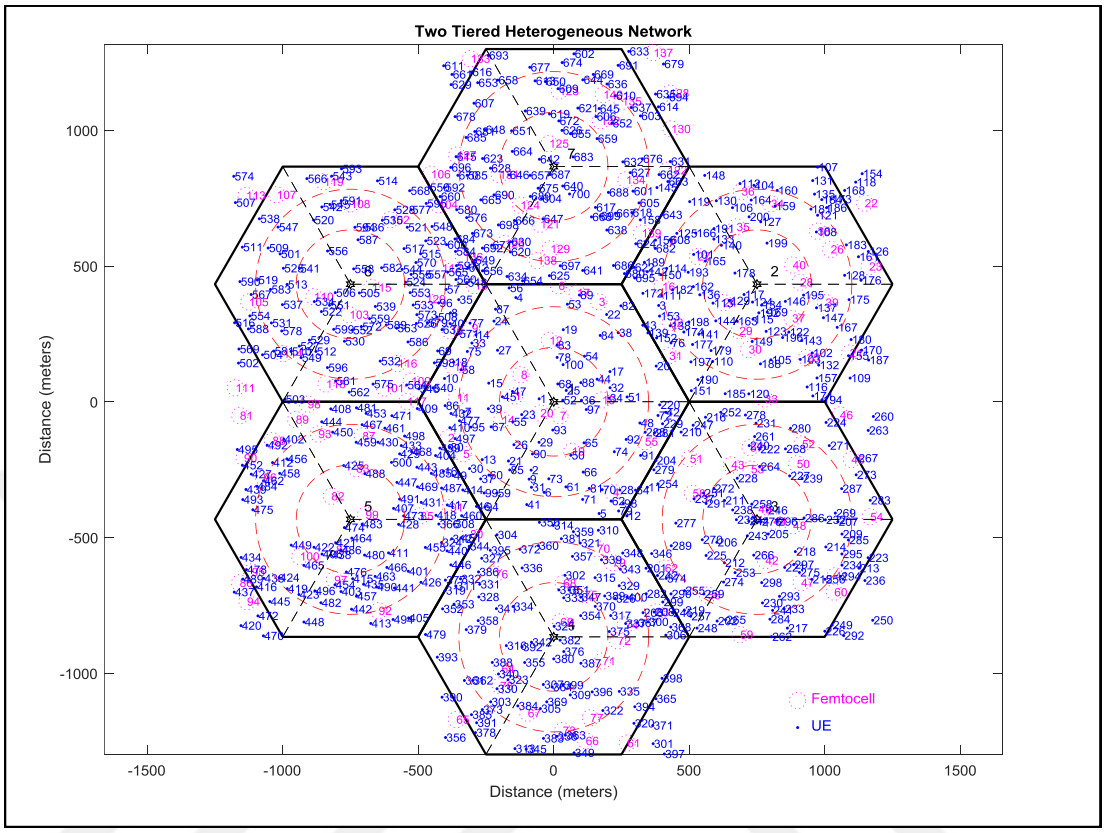

Figure 3.5. Simulation snapshot of a cellular network with 7 macrocells (two-tier)

The simulation results are presented in this subsection, where the proposed FFR-3SL method is compared with the existing FFR methods. The results are presented in Figure 3.6 through Figure 3.11. Throughput achieved by FUEs is given in Figure 3.6. The proposed FFR-3SL method achieves better throughput as compared to the other three existing methods. For all methods, the throughput increases with the increase in number of femtocells. For instance, when the number of femtocells reaches up to 100, the proposed FFR-3SL achieves throughput about 105 Mbps, while FFR-3, FFR-3R, and OSFFR methods achieve around 85, 70 and 60 Mbps of throughput, respectively. The performance gap between the proposed method and other existing methods becomes larger as there are more femtocells deployed in the system. When we consider all the UEs in the system, throughput of our proposed method becomes obviously much larger, i.e, more than twice, than that of other methods as shown in the Figure 3.7. For instance, when the total number of femtocells is 50, the FFR-3SL achieves above 600 Mbps of throughput while at the same number of femtocells, the FFR-3R method has that is half

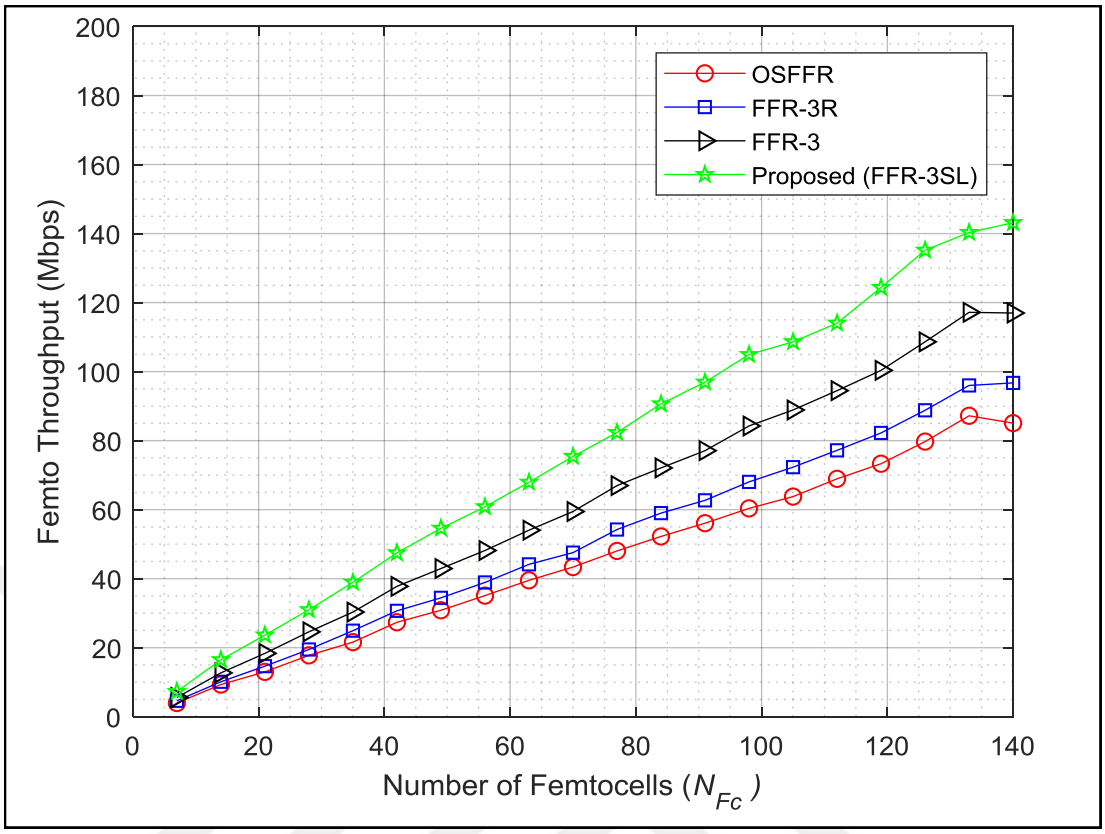

Figure 3.6. Throughput vs no. of femtocells (N_{Fc}) for femto users

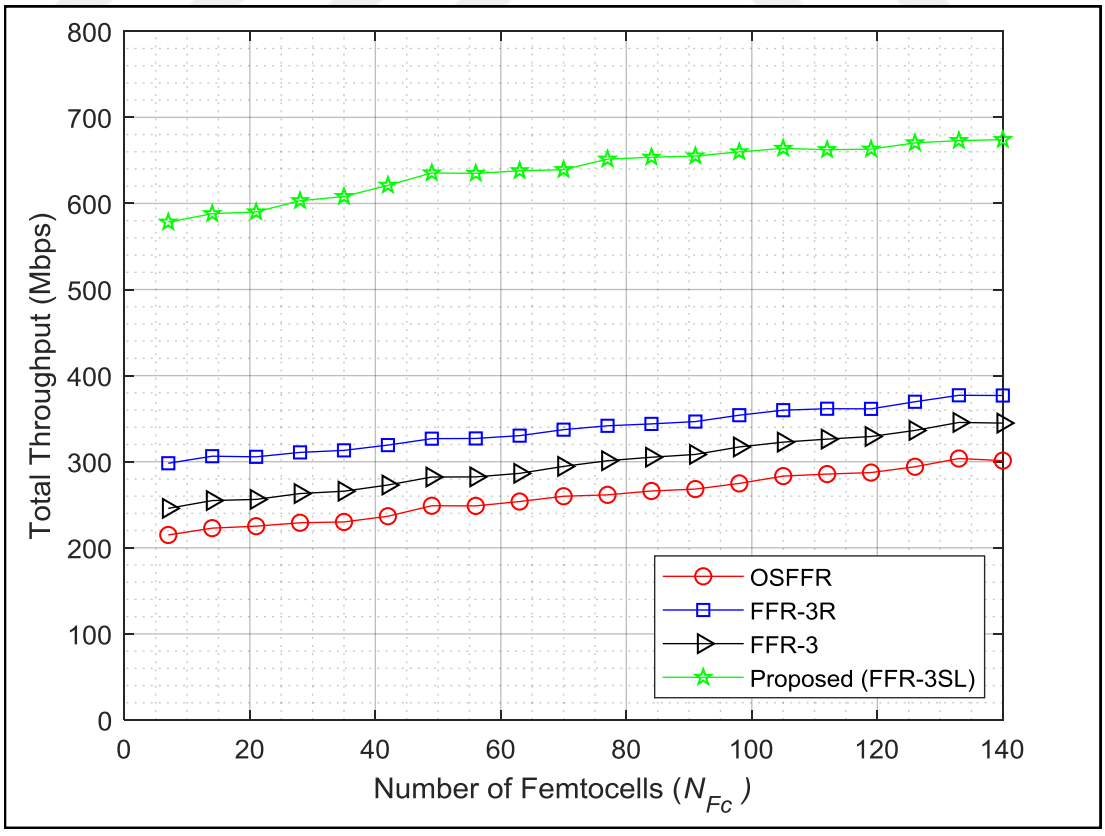

Figure 3.7. Throughput vs no. of femtocells (N_{Fc}) for all users

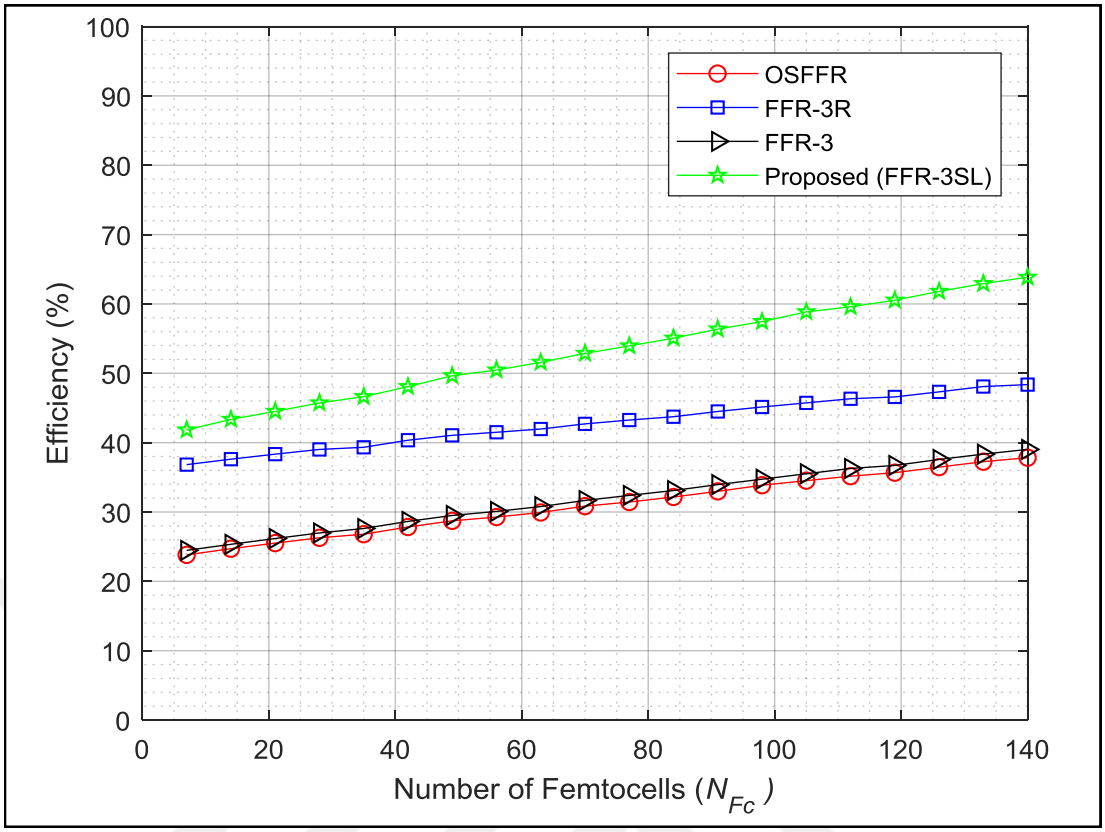

Figure 3.8. System efficiency vs no. of femtocells (N_{Fc})

of the proposed method.

Another performance metric is the efficiency, i.e., UEs connectivity in the system, the results of which are shown in Figure 3.8. As the number of femtocells grows, the percentage of UEs connected to the system in the proposed method is higher than that of other methods. As the total number of femtocells reach up to 140, efficiency of the system in the proposed method approaches to almost 65%, while FFR-3R, FFR-3, and OSFFR methods have efficiencies around 49%, 29%, and 28%, respectively.

The user density distribution in central layer is expressed by,

$$\rho = \frac{N_{UE,c}}{N_{UE}}, \qquad 0 \leq \rho \leq 1. \tag{3.14}$$

where $N_{UE,c}$ and N_{UE} denote the number of UEs deployed in central layer and total number of UEs available in macrocell, respectively. Figure 3.9 presents the results for evaluation the effect of UE distribution in the central layer on the system efficiency for 140 femtocells. When 50% of UEs is deployed in the central layer, the proposed method

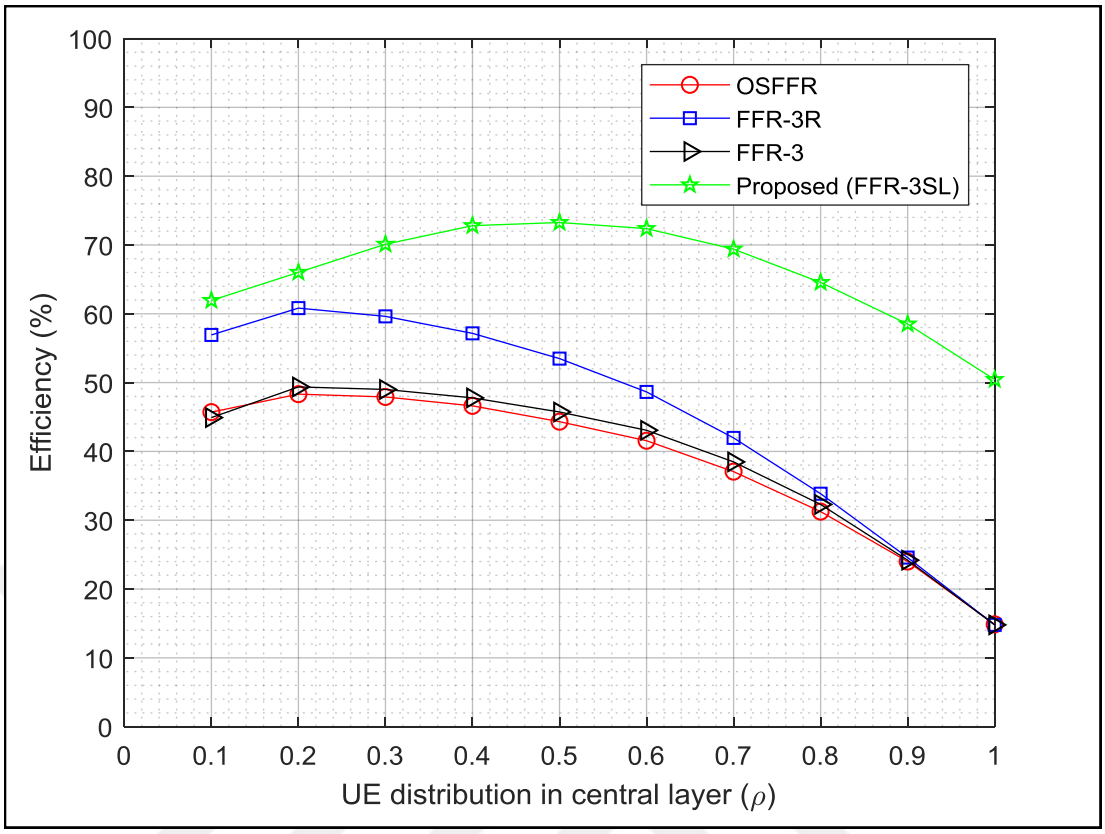

Figure 3.9. The effect of central layer vs system efficiency

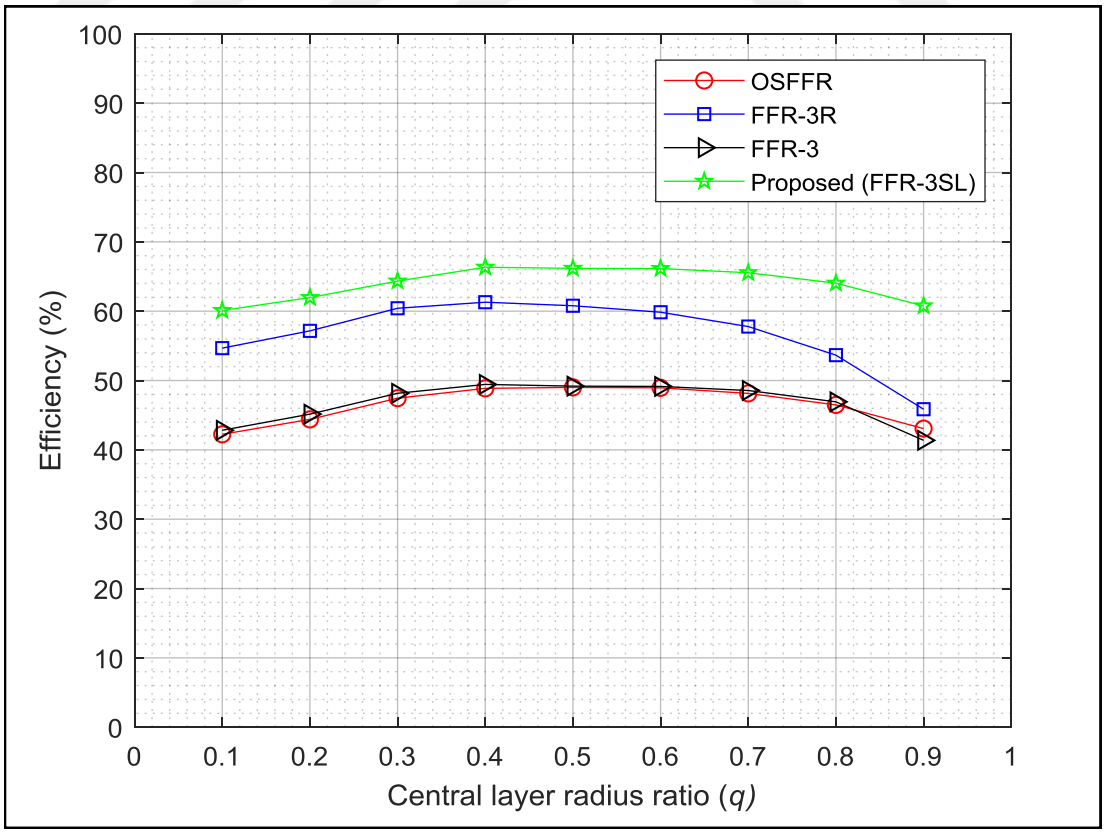

Figure 3.10. The effect of central layer radius vs system efficiency

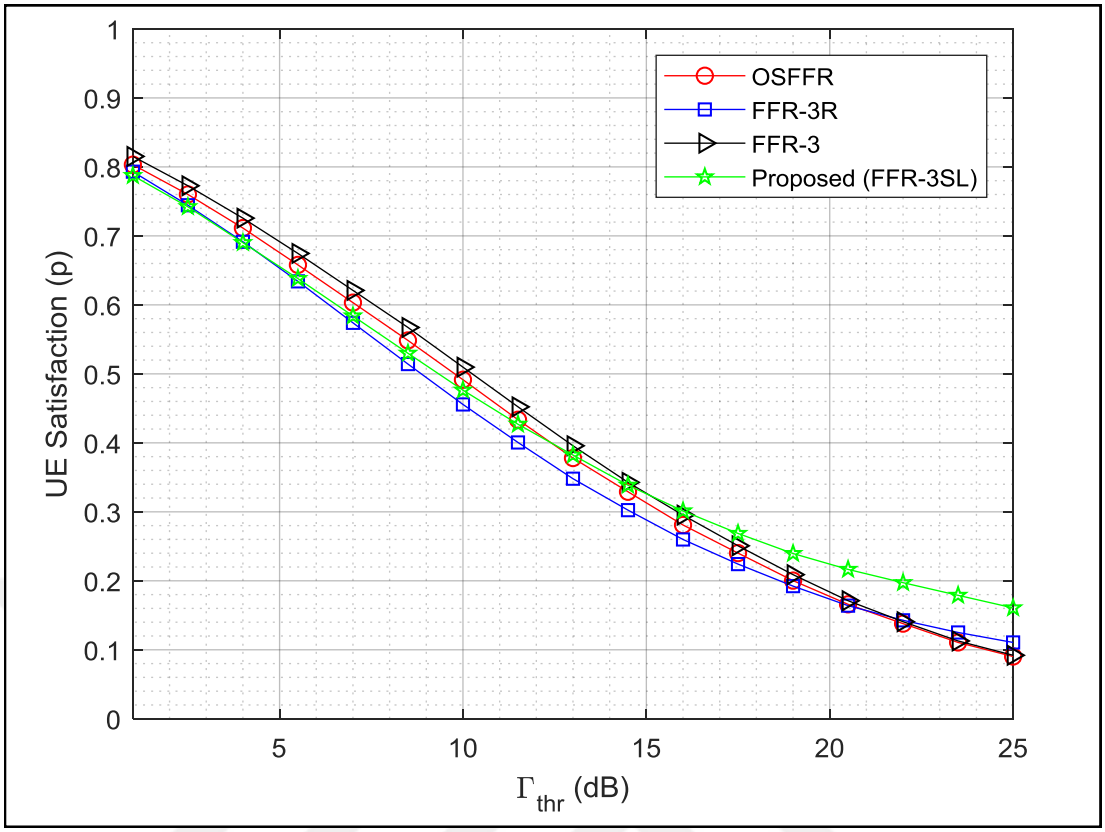

Figure 3.11. The probability of user satisfaction vs SINR threshold

achieves the optimum system efficiency, which is nearly 70% of the overall system. On the other hand, the existing methods FFR-3R, FFR-3, and OSFFR achieve largest system efficiencies of about 60%, 50%, and 48%, respectively, for UE distribution ratio (ρ) of 0.2 in the central layer. This indicates that the methods other than the proposed method focus on the outer layers, while the proposed method mainly focuses on the UEs connected in the center zone. The benefit of the center zone is to give importance to the UEs close to the MBS, which is the main purpose of the HetNet.

In order to investigate the central layer radius on system performance, we define a ratio of central layer radius (r_c) over the whole macrocell radius (R) as,

$$q = \frac{r_c}{R}. \tag{3.15}$$

Figure 3.10 shows the effect of radius of the central layer in a multi-layered HetNet system. All FFR methods achieve optimum efficiency at $q = 0.4$. For instance, at $q = 0.4$, the proposed method achieves the optimum efficiency of about 68%, while the second highest efficiency is achieved by FFR-3R with nearly 62% efficiency. The main idea

of using a variable central layer radius is to be able to change it according to the UEs demand and their location.

Figure 3.11 provides the results regarding UE satisfaction request to varying SINR threshold (Γ_{thr}) values in dB. The UE satisfaction of the proposed FFR-3SL method surpasses all the other existing methods when (Γ_{thr} = 12 dB) and above. Figure 3.11 also shows that the proposed method satisfies almost half of the UEs having SINR threshold value of 10 dB. All the results in the above figures indicate that the proposed FFR-3SL method achieves not only high throughput but also satisfies the UEs regarding SINR thresholds and center layered zones specification.

3.7. Conclusion

In this chapter, the proposed FFR-3SL method for RRM in LTE-A HetNets is explained. FFR-3SL improves the overall throughput of the LTE-A HetNet by controlling the CCI before it occurs. The total available bandwidth is divided into seven subbands, which are then allocated to macrocells and femtocells in different zones of the macrocell coverage areas. In order to implement our new approach for frequency reuse, we proposed a novel FFR-3SL algorithm, which tries to find the best available subband for a newly deployed femtocell in a macrocell coverage area. Moreover, in order to verify the accuracy of the proposed method a Monte Carlo simulation is implemented. Simulation results confirm that the proposed FFR-3SL method reduces not only the CCI but also improves the throughput and efficiency of the overall system. Furthermore, effect of the UEs resource demand, users density distribution, and variation in the central layer radius on the system performance are investigated and compared with three existing methods. Simulation results show that the proposed approach, FFR-3SL outperforms the other FFR approaches for all considered cases.

4. THE EFFECT OF USER LOCATION AND DENSITY ON FFR-3SL

4.1. Introduction

Due to the fast growing rate of subscribers in the cellular network, the operators are approaching from fourth generation (4G) to fifth generation (5G) networks. According to Lina Xu at el. [100] the total number of mobile devices will exceed 50 billion till 2020 and more than 7 trillion devices will be connected to the system every 90 hours [101] where most of the devices will be located inside the buildings. Similarly, a Cisco report [102] says, that by end of 2021, 75% of users will be connected to the core system from inside of the buildings where typical macrocells have weak signals. Therefore, a heterogeneous network (HetNet) comes as a suitable solution for the envisioned 5G mobile cellular networking system which provides better coverage in an indoor environment. Third generation partnership project (3GPP) introduced a HetNet concept in the long term evolution advanced (LTE-A) release-12 specifications. According to 3GPP, HetNet is a multi-tiered network system, where different smallcells are deployed randomly over the existing cellular networks [103]. Smallcells are short-ranged coverage, low powered and easy to plug-in radio access nodes sharing the same licensed frequency bands [104]. The smallcell can consist of relay nodes, microcells, picocells, and femtocells, which are deployed at different places according to user demand and density. One of the significant smallcells is a femtocell, which can be sited at home, offices and public places in order to provide quality services to the indoor subscribers. Sometimes, an femtocell is referred to as Home Evolved Node Base-Station (HeNB) [105]. It covers a relatively short area, i.e., 20 to 30 meters, however, it achieves higher throughput at the UEs. Moreover, HeNBs can be deployed at boundaries to cover the holes and shadow areas of macrocell coverage regions [106]. Furthermore, the most anticipated technologies such as the internet of things (IoTs), etc. in the next 5G will also be benefited from HeNBs in order to connect the home appliances to the core system [107].

Although, HetNet provides higher throughput and better spectral efficiency in urban dense populated areas, however, it creates severe interferences with neighboring femtocells and macrocells [108]. In order to overcome the interferences among femtocells and macrocells, different techniques are presented in the literature [42–45, 91–93]. However, fractional frequency reuse (FFR), which is the most favorable technique to decrease the interference presented in [52–55]. In addition to them, recently we have proposed a new fractional frequency reuse with three sectors and three layers (FFR-3SL) method in [94] to mitigate the co-tier as well as cross-tier interferences in LTE-A HetNets. As a matter of fact, when the size of subbands is fixed then there are chances to waste the radio resources. In this study, an FFR-3SL considering User location and density named as (FFR-3SLU) strategy is presented, in which the radio resources are assigned to the higher density UEs areas in macrocell regions. In FFR-3SL, the whole macrocell coverage area is segmented into three sectors and three layers, which becomes nine zones; while on the other hand, the total available frequency bandwidth is divided into seven frequency subbands (radio resources). According to the FFR-3SLU strategy, the bigger chunk of the frequency band is assigned to the areas that have UEs with high density. Monte Carlo simulation is performed to analyze and examine the performance of the system in terms of throughput and efficiency. Improved throughput and efficiencies are shown in the simulation results when the radio resources are used properly.

4.1.1. Channel model

A downlink wireless propagation channel model is considered, which comprises of path-loss, log-normal shadowing and Rayleigh fading between the evolved node base-station (eNB) and the UE [109]. Moreover, a single wall penetration loss is used from indoor to outdoor transmission and vice-versa, while double wall penetration loss is used among indoor to indoor transmissions.

(a) Path-loss model:

The path loss (PL) between a Femtocell F or Macrocell M and a UE separated by distance d(m) is defined in ITU-R indoor model, the formula is given by,

$$PL(d) = 20\log_{10}(f) + 10N\log_{10}(d) + L_f(n) - 28(dB), \tag{4.1}$$

where the term d is the distance in meters between the transmitter and the receiver, N is the path loss exponent, and $L_f(n)$ is the penetration loss between walls, where n is the factor of walls and the values are,

$$n = \begin{cases} 7dB & d \leq 10m \\ 10dB & 10m \leq d \leq 20m \\ 15dB & d > 20m \end{cases} \tag{4.2}$$

(b) Channel gain:
Assuming a Rayleigh fading channel, the following equation is used to calculate the gain of the channel [110],

$$G = 10^{(-PL+X_\sigma)/10} \times |h|^2 \tag{4.3}$$

where PL is the path loss in dB and X_σ is the shadowing effect of normal distribution. The coherence coefficient, h is complex Gaussian random variable, |h| is the Rayleigh distributed.

4.2. User Location Distribution (ULD) Model

The location of UEs in a macrocell area is a key factor to increase the data rate and spectral efficiency of the system. If the system assigns radio resources to the zones where the number of UEs is high, then we can achieve higher capacity. In this study, we consider a user location distribution (ULD) model used in [111]. In this model, four different cases are discussed such as central layer focused (CLF), middle layer focused (MLF), outer layer focused (OLF), and uniform distribution. Furthermore, the ULDs are set up on the basis of macrocell areas and radius ranges. The radius ranges from the origin are $\delta = \delta_1, \delta_2, ..., \delta_k$. The numbers of UE in a specific area are defined as weighting factors i.e., $\gamma_1, \gamma_2, ..., \gamma_q, \gamma_{q+1}$. The weighting factors are varying during a whole day and the radio resources are assigned accordingly. Nevertheless, the sum of the weighting factors is always equal to unity, i.e $\sum \gamma_i = 1$. To find out the UEs density for

central (U_c), middle (U_m) or outer layer (U_o) in a given cell i the following expression can be used,

$$U = \left\{ U_c, U_m, U_o \right\} = \left\{ \frac{\gamma_c K_{max}}{A_c}, \frac{\gamma_m K_{max}}{A_m}, \frac{\gamma_o K_{max}}{A_o} \right\} \tag{4.4}$$

where $A_c = \pi(\delta_1^2 - \delta_{min}^2)$, $A_m = \pi(\delta_2^2 - \delta_1^2)$ and $A_o = 3\sqrt{3}(\delta_{max}^2/2 - \pi\delta_2^2)$ are the areas of central, middle and outer layers, respectively. Moreover, γ_c, γ_m, and γ_o represent density of central, middle and outer layer, respectively. The user location distribution is given in Table 4.1.

Table 4.1. The ratio of user location distribution in different layers

Focused Layer	U_c **(%)**	U_m **(%)**	U_o **(%)**
Central Layer Focused	25	50	25
Middle Layer Focused	25	50	25
Outer Layer Focused	25	25	50
Uniform Distribution	33	33	33

Following we discuss the four different ULD classes.

4.2.1. Central layer focused (CLF):

50% of the UEs are located in the central layer while the remaining 50% of the UEs are randomly distributed in the middle and outer layers of the macrocell.

4.2.2. Middle layer focused (MLF):

50% of the UEs are positioned in the middle layer while the other 50% of the UEs are randomly distributed among the central and outer layers of the macrocell.

4.2.3. Outer layer focused (OLF):

50% of the UEs are placed in the outer layer while the rest 50% of the UEs are randomly distributed among the middle and outer layers of the macrocell.

4.2.4. Uniform distribution:

All the UEs are uniformly distributed across all layers in the macrocell region.

4.2.5. Scenarios

We considered three different scenarios to examine the effect of FFR-3SLU in terms of throughput and efficiency in the LTE-A HetNet system. The comparison of user density is given in Table 4.1.

Scenario A:
By considering the CLF case, half of the radio resources (no. of RBs) are assigned to the subband (G) which is serving in the central layer, while the remaining radio resources are shared among all other subbands.

Scenario B:
By considering the MLF case, 50% of the radio resources are allotted to the middle layer's subbands (A, B, C), while the remaining radio resources are shared among all other subbands.

Scenario C:
In a similar manner, by considering the OLF case, half of the radio resources are issued to the subbands serving in the outer layer, such as (D, E, F), while the remaining radio resources are shared among all other subbands. The flowchart of the proposed FFR-3SL method is given in the Figure 4.1.

4.3. Performance Evaluation Metrics

4.3.1. Signal to interference and noise ratio (SINR)

The downlink SINR values received at the UE in an LTE-A network are heavily effected due to interference that occurs among femtocells and macrocells. In LTE-A HetNets the interferer signals are also received from undesired transmitters in the downlink channel. Considering the macrocell M, macro UE (MUE) m and subcarrier k, the equation to calculate the SINR [112] is defined as,

$$\mathrm{SINR}_m^k = \frac{P_M^k G_{m,M}^k}{N_o \Delta f + \sum_m P_{M'}^k G_{m,M'}^k + \sum_m P_F^k G_{m,F}^k} \tag{4.5}$$

where P_M^k, $G_{m,M}^k$ indicate the transmit power and the channel gain of a MUE m from the desired macrocell M at subcarrier k respectively. In denominator, N_o is the noise

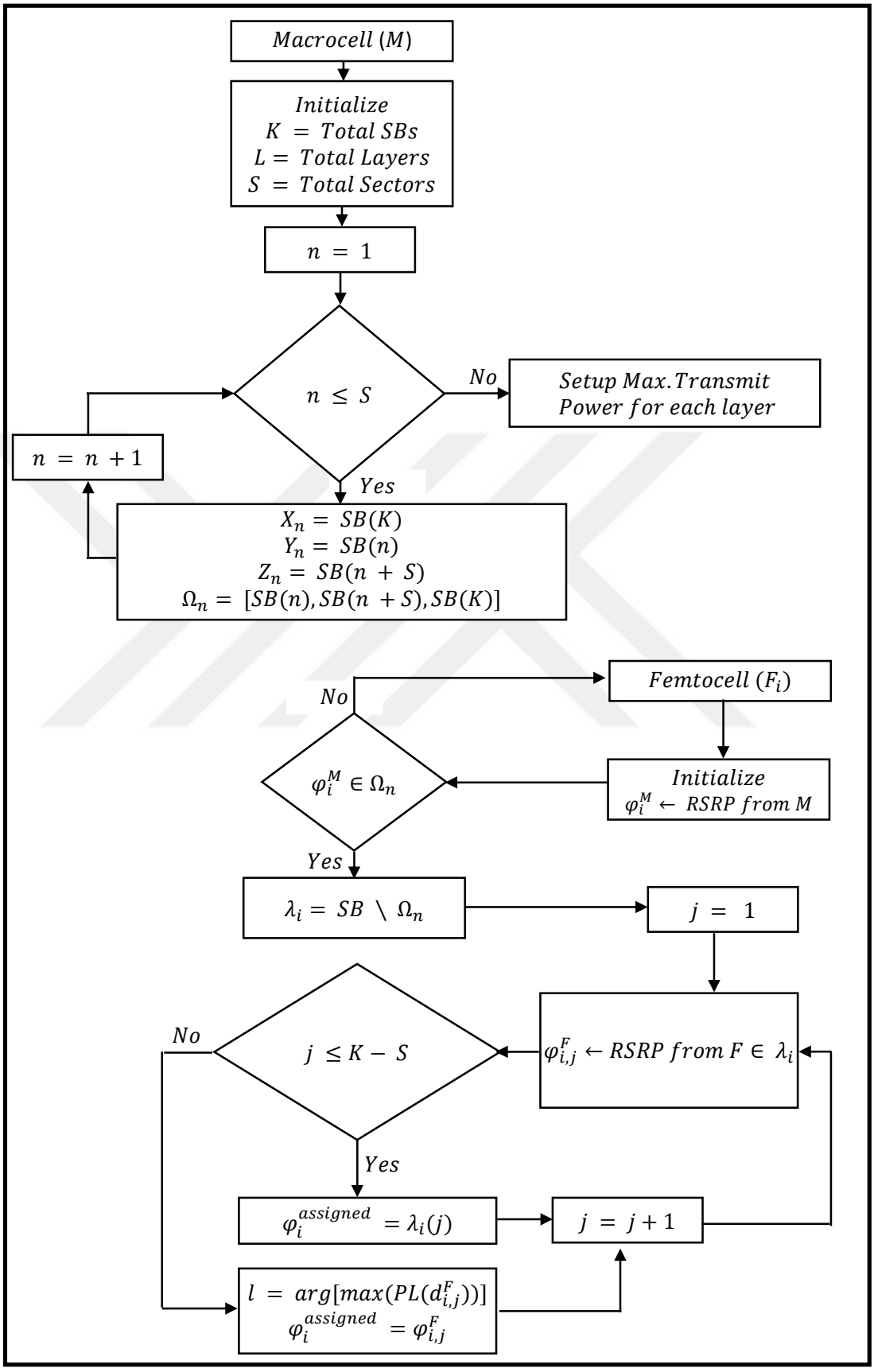

Figure 4.1. A flowchart of the proposed FFR-3SL algorithm

spectral density of subcarrier spacing Δf. The $P^k_{M'}$ and $G^k_{m,M'}$ are the transmit power and channel gain at subcarrier k of a MUE m from the undesired macrocells M′. While, the P^k_F and $G^k_{m,F}$ are the transmit power and channel gain at subcarrier k of a MUE m from the unwanted femtocells F.

Similarly, we obtain the SINR value from femtocell F at the subcarrier k of a Femto UE (FUE) f, the equation is described as,

$$SINR^k_f = \frac{P^k_F G^k_{f,F}}{N_o \Delta f + \sum_f P^k_{F'} G^k_{f,F'} + \sum_f P^k_M G^k_{f,M}} \tag{4.6}$$

where P^k_F, $G^k_{f,F}$ indicate the transmit power and the channel gain from the desired femtocell F at subcarrier k of a FUE f respectively. The $P^k_{F'}$ and $G^k_{f,F'}$ are the transmit power and channel gain at subcarrier k of a FUE f from the undesired femtocell F′. Similarly, the P^k_M and $G^k_{m,M}$ are the transmit power and channel gain at subcarrier k of a FUE f from the macrocell M.

4.3.2. Channel capacity

As known, the Shannon capacity of the system depends on SINR value and the bandwidth of the subband. The channel capacity is computed by using the following equation [113],

$$C^k_x = \Delta f \times \log_2(1 + \alpha SINR^k_x), \qquad x \varepsilon \{m, f\}. \tag{4.7}$$

where, $SINR^k_x$ is the SINR (dB) value of UE m at subcarrier k, and $\alpha = -1.5/\text{In}(5\text{BER})$. BER stands for the target bit error rate.

4.3.3. Throughput

The throughput T_X, $X \varepsilon \{M, F\}$ achieved by a macrocell M and a femtocell F can be written as,

$$T_X = \sum_x \sum_k \psi^k_x C^k_x, \qquad X \varepsilon \{M, F\}, \quad x \varepsilon \{m, f\}. \tag{4.8}$$

where ψ_x^k indicates the subcarrier k assignment to UE x. When $\psi_x^k = 1$, it indicates that the subcarrier k is assigned to UE x, otherwise, $\psi_x^k = 0$.

Total throughput of the system is obtained by summing up the throughputs achieved by femtocells F and macrocells M,

$$T_{total} = T_M + T_F. \quad (4.9)$$

4.4. System Level Performance

In order to assess the overall performance of the system, we used LTE-A system parameters and values. The details descriptions are given in the following subsections.

4.4.1. Network parameters

Table 4.2. Network parameters for FFR-3SLU implementation

Parameters	**Values**
Channel Bandwidth	20 MHz
Carrier Frequency	2.0 GHz
Sub-carrier spacing (Δf)	15 KHz
Total number of RBs	100
Macrocell Radius	500 m
Femtocell Radius	30 m
Total no. of Macrocells	7
Total no. of Femtocells	140
No. of Femtocells per Macrocell	20
Max. no. of UEs per Femtocells	5
Number of UEs per Macrocell	100
Macrocell Transmit Powers	[20 , 15 , 10] Watt
Femtocell Transmit Power	20 mWatt
White Noise Power Density	-174 dBm/Hz
Target BER	10^{-6}

A Matlab level simulation tool is used to assess and analyze the performance of the above mentioned scenarios. The major network parameter values are listed in Table

4.2. For obtaining reasonable results, an LTE-A two-tiered HetNet is adopted which consists of 7 macrocells and a total of 140 femtocells which are uniformly distributed across the macrocell regions. Moreover, a total of 100 UEs are considered per every macrocell region which are distributed in proportion to the ULD scenarios. After setting up the network parameters, the Monte Carlo simulation is performed 100 times to obtain adequate results.

4.4.2. Simulation results

The results from Figure 4.2 through 4.7 are obtained by considering the ULD based FFR strategy under the FFR-3SL Model. Moreover, the above mentioned (in Section-III) three scenarios are applied to get these results. Figure 4.2 and 4.3 are obtained by considering Scenario A. In these figures the total throughput and efficiency are displayed, respectively. It is shown that CLF achieves higher throughput and better efficiency as compared to other layers where there is no ULD strategy is applied.

Similarly, by using Scenario B Figure 4.4 and Figure 4.5 are obtained. The figures show considerably higher throughput and quite better efficiency when it compares with the previous scenario. In the previous scenario, the maximum efficiency and throughput achieved by MLF were 88% and 250 Mbps, respectively, when there was no ULD approach used. When the ULD technique applied then the efficiency and throughput are improved up to 10% of the total values.

Figure 4.6 and 4.7 are plotted when Scenario C is considered. It clearly shows that efficiency progresses well when compared with the previously scenarios; while on the other hand, the throughput of the system slightly increases. The reason is that many UEs are deployed at the edges of the macrocell where they receive weak signals. Therefore, it is highly recommended that femtocells or relay nodes should be deployed at the boundaries of macrocell in order to achieve higher throughput and capacity of the system.

Finally, we observe that the user densified layers achieve higher throughput and better efficiency if the radio resources utilize efficiently. The populated areas should be given a bigger chunk of a subband from the available bandwidth.

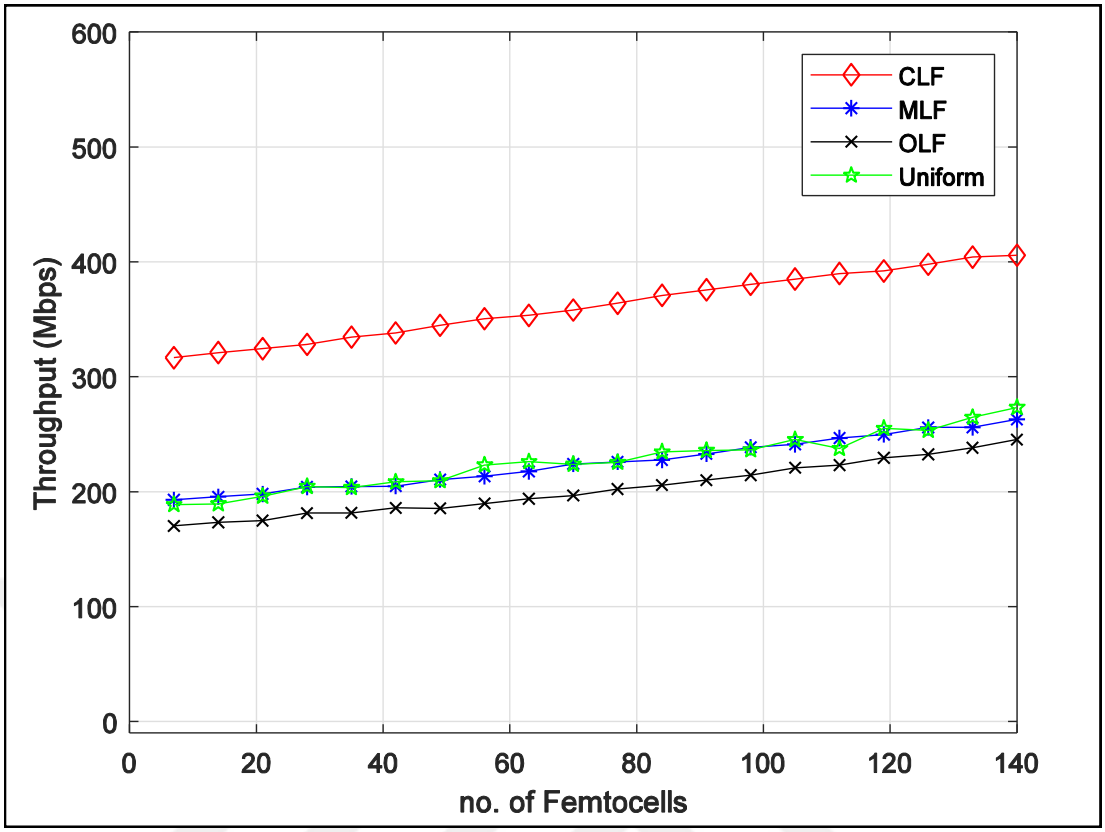

Figure 4.2. Throughput vs no. of femtocells for scenario A

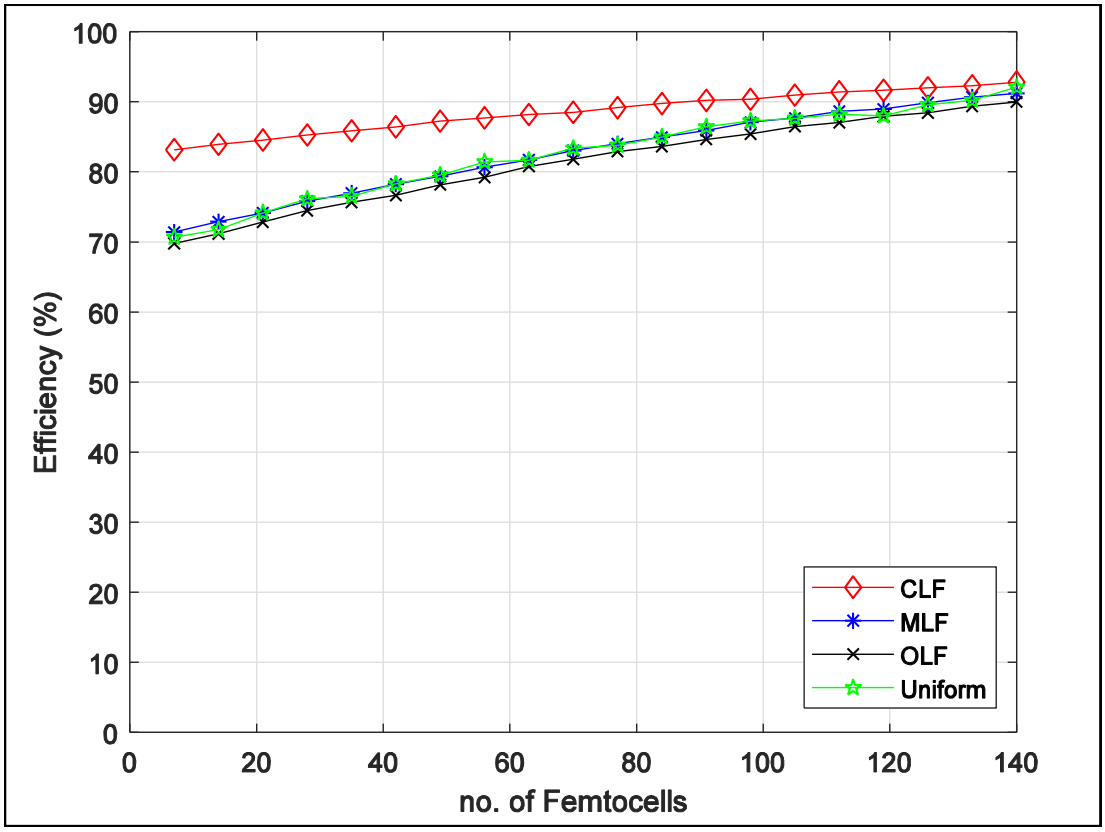

Figure 4.3. Efficiency vs no. of femtocells for scenario A

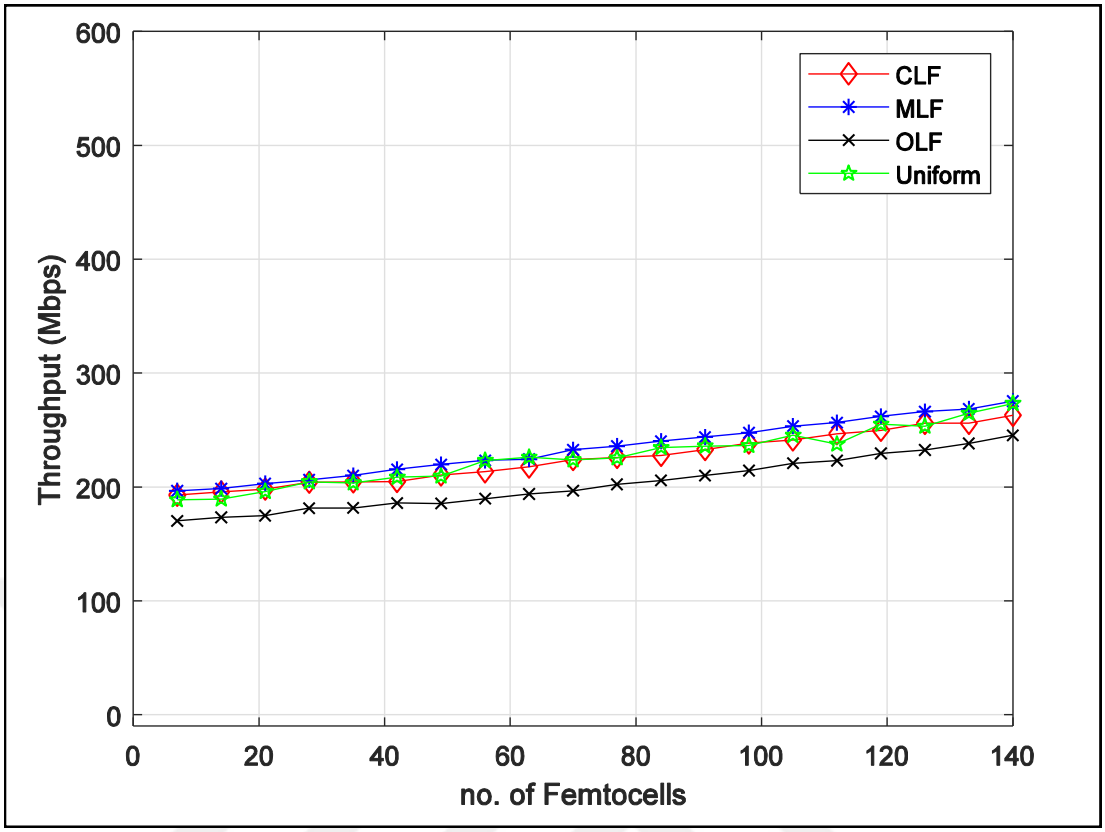

Figure 4.4. Throughput vs no. of femtocells for scenario B

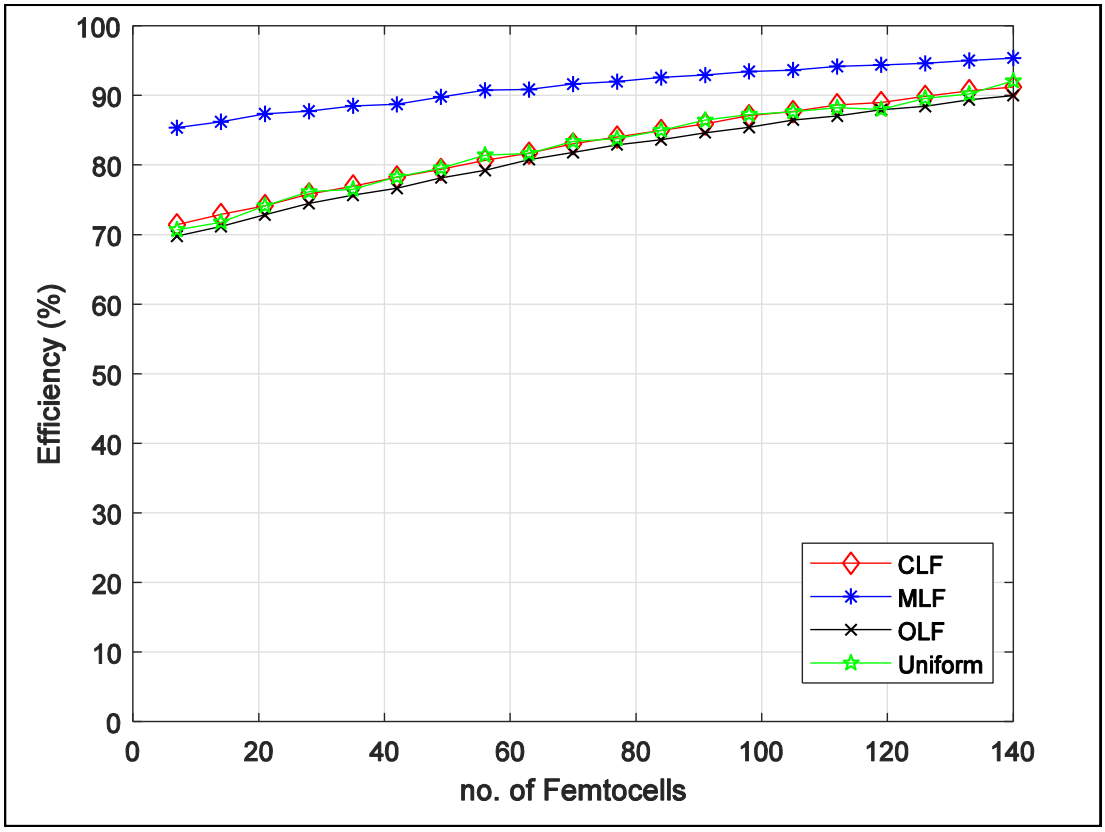

Figure 4.5. Efficiency vs no. of femtocells for scenario B

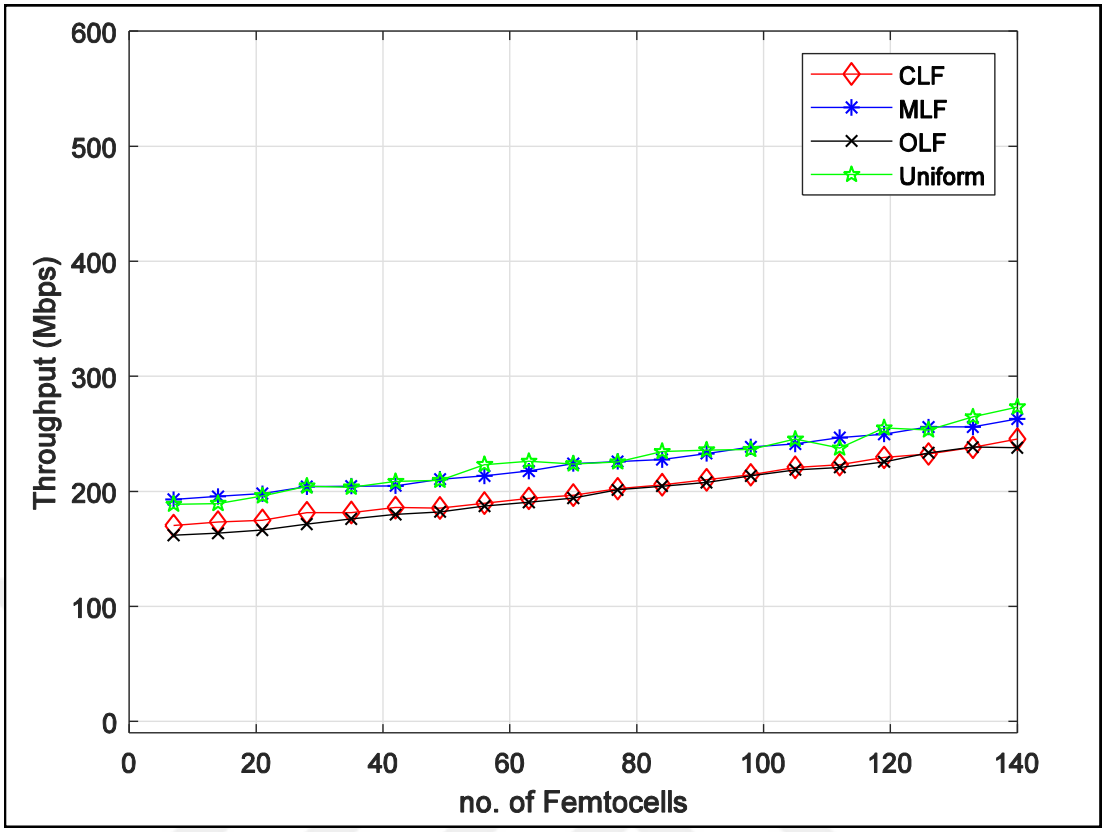

Figure 4.6. Throughput vs no. of femtocells for scenario C

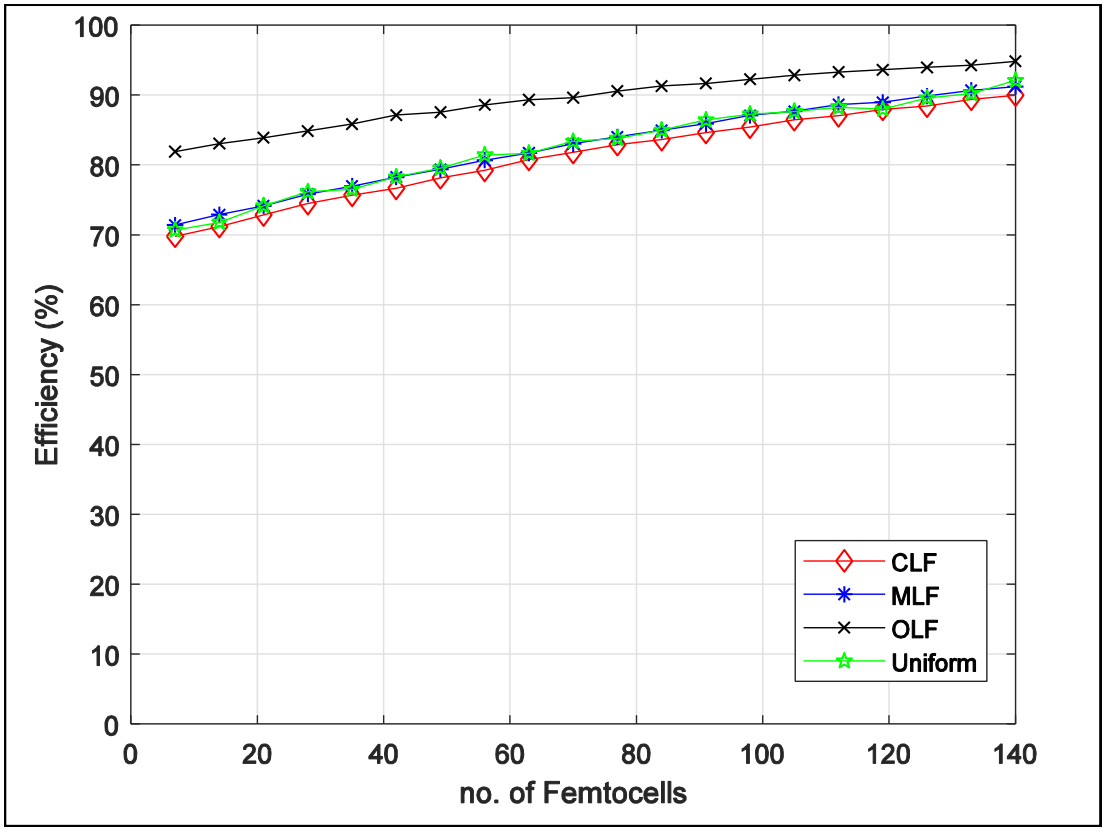

Figure 4.7. Efficiency vs no. of femtocells for scenario C

4.5. Conclusion

In this chapter, a new FFR-3SLU strategy is presented, which utilizes the radio resources (subbands) efficiently according to the user location distribution (ULD) in LTE-A HetNets. The total available bandwidth is divided into seven subbands while the size of a subband depends on the UEs demand and density in a layer. As a result, the overall throughput of the LTE-A HetNet system can be maximized by managing the radio resources properly. The simulation results showed, that the assignment of a bigger chunk of a subband to the high densified area achieves higher throughput and better efficiency. In this study, a uniform distribution of femtocells is considered; however, in future work, a proper femtocells deployment strategy will be considered to increase the overall throughput of the LTE-A HetNet systems.

5. POWER CONTROL MECHANISM FOR LTE-A HETNETS

5.1. Introduction

The number of portable devices and home appliances need a robust connectivity to the so-called fifth generation (5G) technology. On the other hand, the mobile subscribers are growing rapidly which also demand for high data rates. Figure 5.1 shows the Ericsson report predicted the yearly increase subscribers [1]. The report indicates that until 2025 the number of mobile broadband subscriptions will reach up to nine billion, where almost eight billion people will connect to system from indoor environment. Furthermore, the smartphone data and video data traffic will increase up to 20 and 25 times respectively. Another report issued by Cisco, where estimated that around 11 Exabyte data per month is used by the mobile subscribers in 2017 and expecting that 49 Exabyte data per month will be used till 2021 [2].

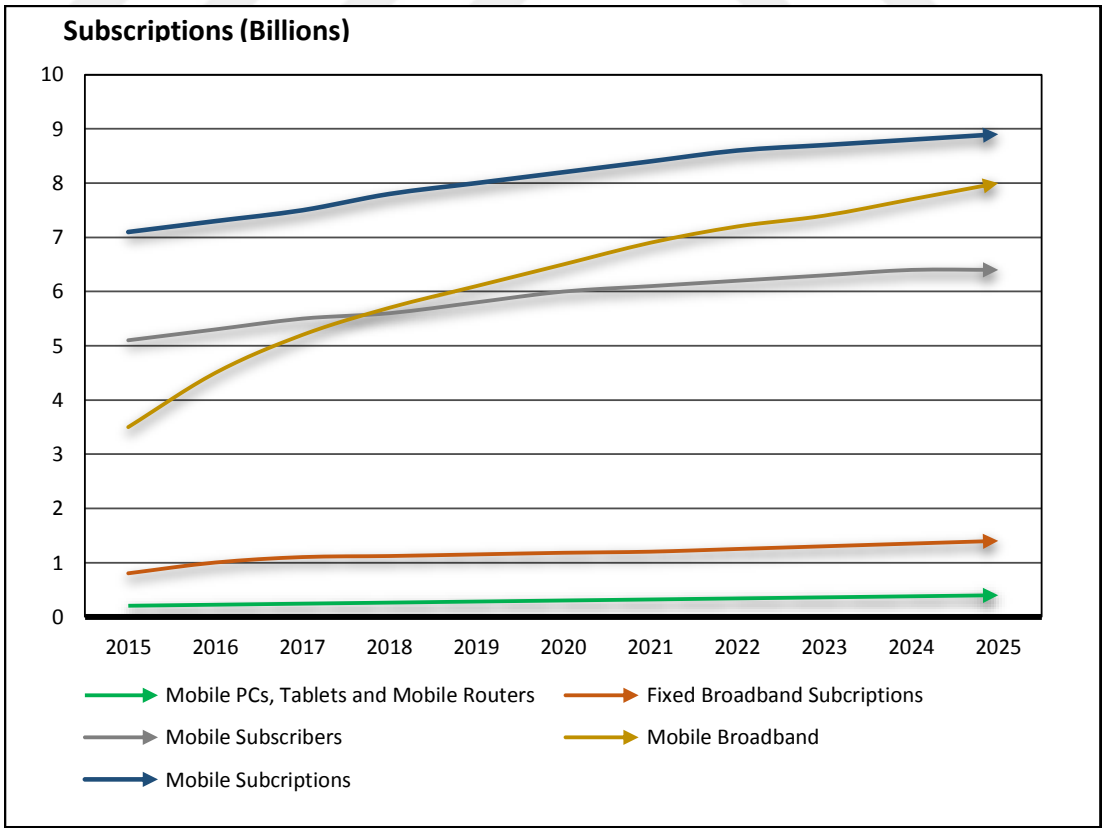

Figure 5.1. Yearly growth of mobile subscribers published by Ericsson

In 2008, the third generation partnership project (3GPP) came up with a new technology called Long Term Evolution (LTE) in Release-8 and later in 2010, it is called LTE Advanced (LTE-A) in Release-10. LTE-A is a state of the art technology which provides above 1 Gbps downloading and about 500 Mbps uploading data rates [3]. However, the recent LTE-A system is totally based on typical homogeneous cellular concept, where the whole cell is covered by a macrocell antenna which is known as evolved node base-station (eNB) in LTE standards. These eNBs use the same transmission power, modulation techniques, access methods, and antenna patterns [4] and guarantee quality of service (QoS) to the end user equipment (UE) across the whole coverage area [5]. On the contrary, the UEs at edges or in congested areas suffer from weak signal powers; as a result, the capacity and data rates are reduced in those areas. First solution to tackle these problems is to shrink the radius of the macro cells and deploy more eNBs in the urban congested or weak signal areas, however this approach is costly and needs extra investment [6]. Therefore, the heterogeneous networks (HetNets) emerge as one of the most auspicious improvements toward realizing the objective specifications of LTE-A networks. It is expected, that this approach will improve the system capacity and increase the coverage and capacity of the cell in a cost-effective way [7].

There are many techniques adopted to improve or reduce the interferences issues in LTE-A heterogeneous networks (HetNets). The transmit power control mechanism can be considered as one of the easiest and beneficial techniques to overcome the interference issues in LTE-A HetNets. In this Chapter, we discuss the transmit power control mechanism and propose an algorithm named power control algorithm (PCA) to reduce the interference among macro cells and femtocells either in uplink or downlink transmission channel. In this technique, the system uses the signal to interference and noise ratio (SINR) and reference signal received power (RSRP) to calculate the signal power level for downlink and uplink, respectively. A serving gateway is used to control the switching of UE among macro cells and femtocells on the basis of the signal strength received. A MATLAB simulation [13] is used to analyze the effect of PCA in LTE-A HetNets.

5.2. System Model and Analysis

The entire LTE-A network is Internet Protocol (IP) based which is capable of transferring voice, video and data traffic reliably and securely. The core principle behind using IP to dynamically assign the address when mobile is switch on and release when it is switched off. In LTE-A, to achieve high data rates, the subcarriers are shared by many users in OFDMA [14]. Due to the complex processing, OFDMA needs more power to calculate, and that is why Single Carrier- Frequency Division Multiple Access (SC-FDMA) is used on the UE side because of less complexity [15].

5.2.1. Measurement scales

The analysis of Radio Frequency (RF) value is essential in wireless broadcasting and communications system because these values indicate the condition and performance of the system. There are some ranges of RF values, which have to be considered while measuring the performance of the system. Table 5.1 depicts a useful classification of RF status vs. LTE key performance indicators (KPIs). The Evolved UMTS Terrestrial Radio Access Network (EUTRAN) compiled the data in this chart during RF turning process and distributed among all the major LTE-A operators [16]. There might be several other tables exist, but the results are almost similar in large extent. All LTE-A significant vendors use the following quantities for RF signal measurements.

- Signal to Interference and Noise Ratio (SINR)
- Reference Signal Received Power (RSRP)
- Reference Signal Received Quality (RSRQ)

Table 5.1. Classification of RF condition vs. LTE-A KPIs

Condition	**SINR (dB)**	**RSRQ** (dB)	**RSRP (dBm)**
Excellent	≥ 20	≥ -10	≥ -80
Good	13 to 20	–10 to –15	–80 to –90
Cell Middle	0 to 13	–15 to –20	–90 to –100
Cell Edge	≤ 0	≤ -20	≤ -100

5.2.2. LTE-A measurement metrics

The management of interference in LTE-A femtocells is more critical than the conventional macro cellular networks because femtocells use the same frequency spectrum as the used by the macrocells. In 3GPP specifications, the uplink and downlink signals strength are calculated as RSRP and SINR values, respectively. The SINR to RSRQ conversion is described as below,

$$\text{SINR} = \frac{\text{S}}{\text{I}+\text{N}} \tag{5.1}$$

where S is the power of the signal, I is the interference level, and N is the background noise. These measurements are obtained when the same frequency bands used.

According to 3GPP, the RSRQ is defined as,

$$\text{RSRQ} = \text{N}_{\text{prb}} \frac{\text{RSRP}}{\text{RSSI}} \tag{5.2}$$

where received signal strength indicator (RSSI) used by UEs, and N_{prb} is the number of Resource Blocks (RBs). In OFDM system, the self interference of a cell is often avoided, therefore, the other interferences are weighed as I.

$$\text{RSSI} = \text{S} + \text{I} + \text{N} \tag{5.3}$$

where S is the signal power strength of 12 sub-carriers, I is the interference received from nearby cells, and N is the Additive White Gaussian Noise (AWGN). The absolute power received from 12 sub-carriers depends on the OFDM symbols rate, as given by,

$$S_{tot} = \rho \times 12 \times N_{prb} \times RSRP \tag{5.4}$$

$$\rho = \frac{RE}{RB}, \qquad RE = 15KHz \tag{5.5}$$

If all the subcarriers are transmitted for an OFDM symbol, then $\rho = 1$. On the other hand, interference and noise power are represented as,

$$I + N = \frac{I_{tot} + N_{tot}}{12 \times N_{prb}} \tag{5.6}$$

where I_{tot} indicate the total interference while N_{tot} is the total noise power. Now substituting the values of equation 5.4 and equation 5.6 into equation 5.1, we get,

$$SINR = \frac{\rho \times N_{prb} \times RSRP}{I_{tot} + (N_{tot}/12) \times N_{prb}} \tag{5.7}$$

After simplification of the equation 5.7, the SINR can be obtained as,

$$SINR = \frac{12N_{prb} \times RSRP}{I_{tot} + N_{tot}}, \tag{5.8}$$

Now, using equation 5.3, we obtain,

$$SINR = \frac{12N_{prb} \times RSRP}{RSSI - S_{tot}}, \tag{5.9}$$

After modification of equation 5.2, we can get the value of RSSI and insert in equation 5.9. Also, by inserting the values of equation 5.4. The SINR is given by,

$$SINR = \frac{12N_{prb} \times RSRP}{N_{prb}\frac{RSRP}{RSRQ} - x \times 12N_{prb} \times RSRP}, \tag{5.10}$$

Finally, we can get the value of SINR from the above equations,

$$SINR = \frac{1}{\frac{1}{12 \times RSRQ} - \rho}. \tag{5.11}$$

5.3. System Design

5.3.1. Topology

The 3GPP LTE-A specify macrocell in [17] which is also known as eNB and femtocell is mentioned as HeNB , which are capable of transmission and reception of signals in one or more cells. In Figure 2.2, the general 3GPP system specification of HetNet and EPC are demonstrated. The HeNBs are connected with the HeNB gateway, and then HeNB gateway is linked to the EPC of the core system [12]. However, Figure 5.2 describes the overall scenario that we focused on during this study. For instance, we used a macrocell, two femtocells, four femtocell UEs (FUE) and two macrocell UEs (MUE).

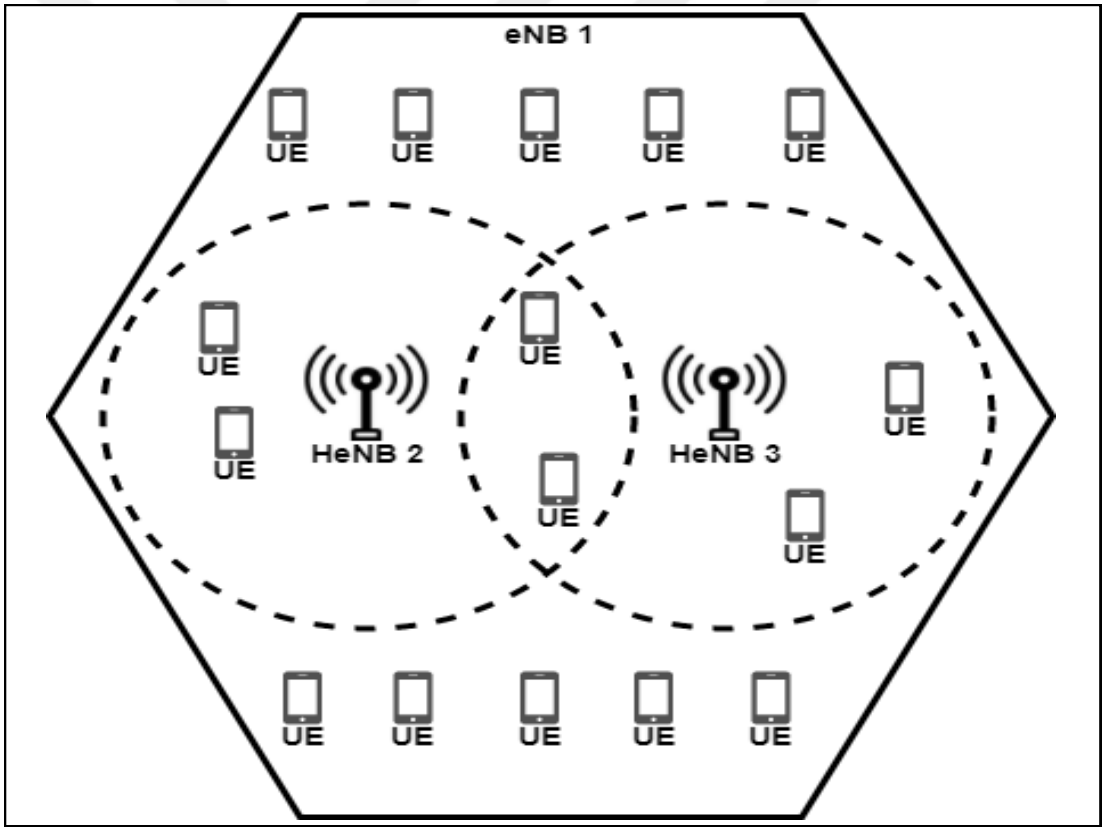

Figure 5.2. Two-tiered HetNet topology

5.3.2. System flowchart

In this section, we implemented a femtocell and macrocell simulator, which is freely available at [18]. This simulator is used to perform the power control algorithm and to find out the maximum power level in the existing HetNets. Primarily, the proposed PCA

algorithm is reasonably separated two layers. One layer is working on the back-end and calculate the values of RSRP and SINR, while the front-end layer displays the overall performance of the system. Figure 5.3 is the flowchart of the proposed power control mechanism, which is carried out for the performance measurements of the LTE-A HetNet system.

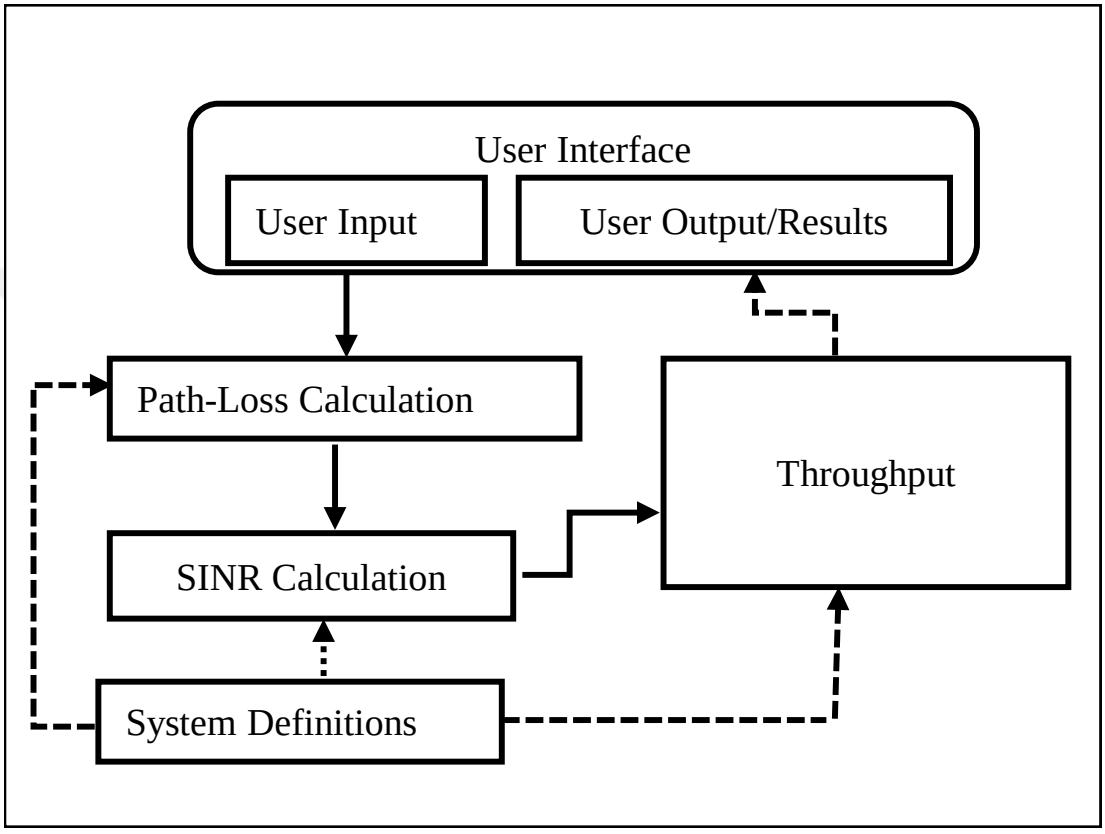

Figure 5.3. Flowchart of the proposed power control mechanism

5.4. Simulation Setup

Based on the previous discussions and formulations, we set up the simulator as mentioned in [18]. This simulator is very easy to use and has a user-friendly display. The researchers can modify the code according to the requirements. To obtain useful results we set the positions and values of the cells used in this work.

5.4.1. Main layout

The main layout of the simulator provides the visual display facility for placing and organizing the femtocells inside the central macrocell. Figure 5.4 shows the initial window, where the user can set the number of femtocells and the number of UEs

connected with femtocells or macrocell. Here the user can also set the parameters to obtain the results accordingly.

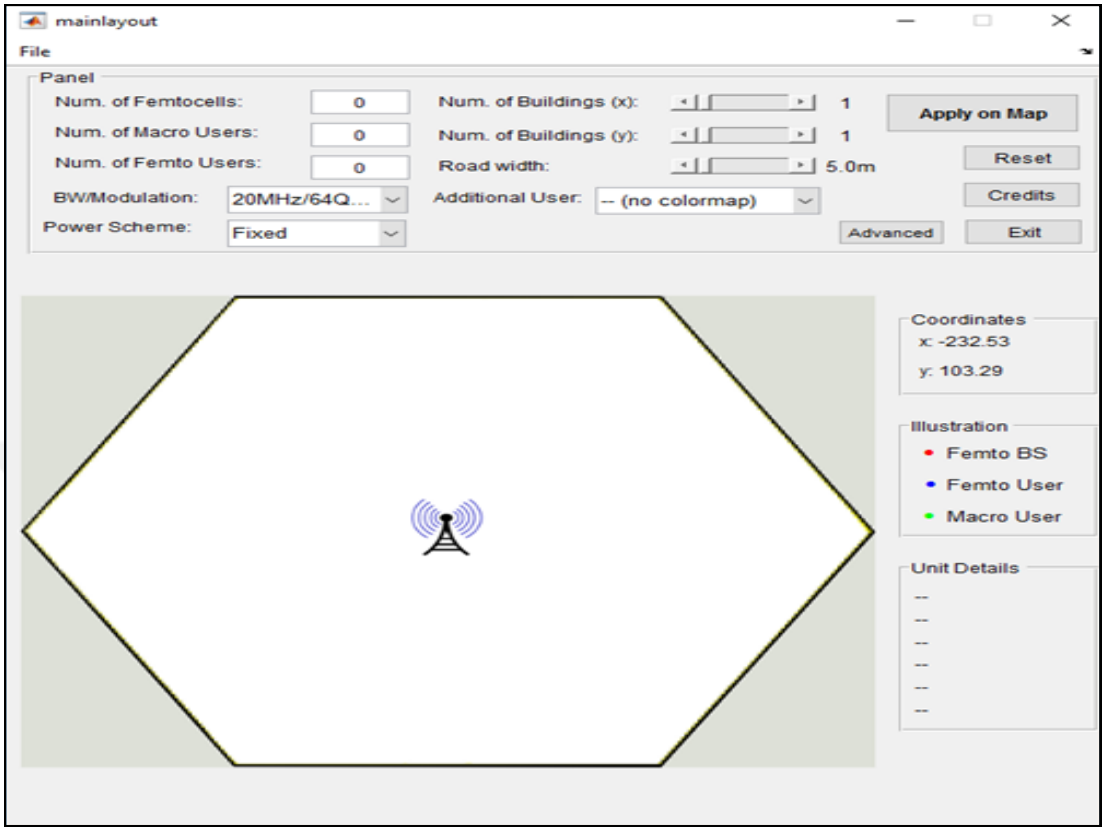

Figure 5.4. Main layout of the simulator for LTE-A HetNet

5.4.2. Simulation parameters for LTE-A HetNet

As stated above, there are different options available to set up the values according to the requirements. Table 5.2 shows the parameters which are used during the LTE-A HetNet simulation. The values are set before running the simulation. LTE-A can be operated on many different frequency bandwidth, however, we used 10 MHz. First of all, the radius of both macrocell and femtocells are selected.

Table 5.2. Simulation parameters for LTE-A HetNet

Parameters	**Value**
Macrocell Coverage Area	250 m
Femtocell Coverage Area	20 m
Carrier Frequency	2 GHz
Macrocell Transmit Power	45 dBm
Femtocell Transmit Power	20 dBm
Number of Macrocells	1
Number of Femtocells	2
Outdoor Wall Loss	20 dB
Indoor Wall Loss	5dB
Bandwidth	10 MHz
Modulation	QPSK
Subcarrier Spacing	15 KHz

5.5. Simulation Results

In an initial step, the location of femtocells and UEs are randomly located. The specific values for generating the scenarios of rearranging the particular position of femtocell and UEs are entered, and the action of the "Apply The Map" is applied. Figure 5.5 illustrates the detail graphical overview of the network with particular positions of femtocells and UEs. Furthermore, the coordinate's points (x,y), power schemes, modulation techniques and other detail are also mentioned. In next step, the "Run Simulation" is selected for generating the result. In Figure 5.6, we can analyze the power level of the downlink signal from lowest to the highest value. The maximum power value of the selected unit indicates the position and throughput received at the UE. If the UE is near to femtocell, it will receive the high power of the signal, and when it moves far away from the femtocell, the signal power level will decrease to the minimum level. When the UE receives another signal from nearby femtocell or macrocell, then the two received signals power would be compared according to the equation 5.11.

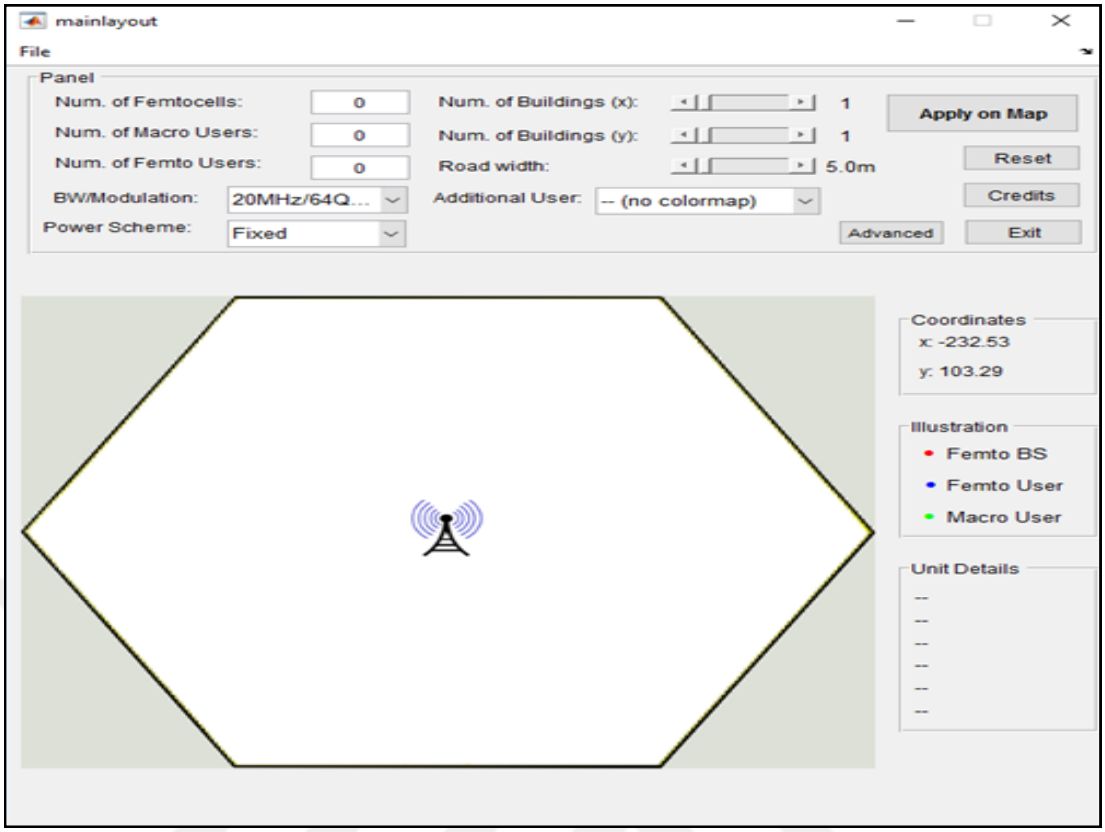

Figure 5.5. Simulation configuration setup for LTE-A HetNet

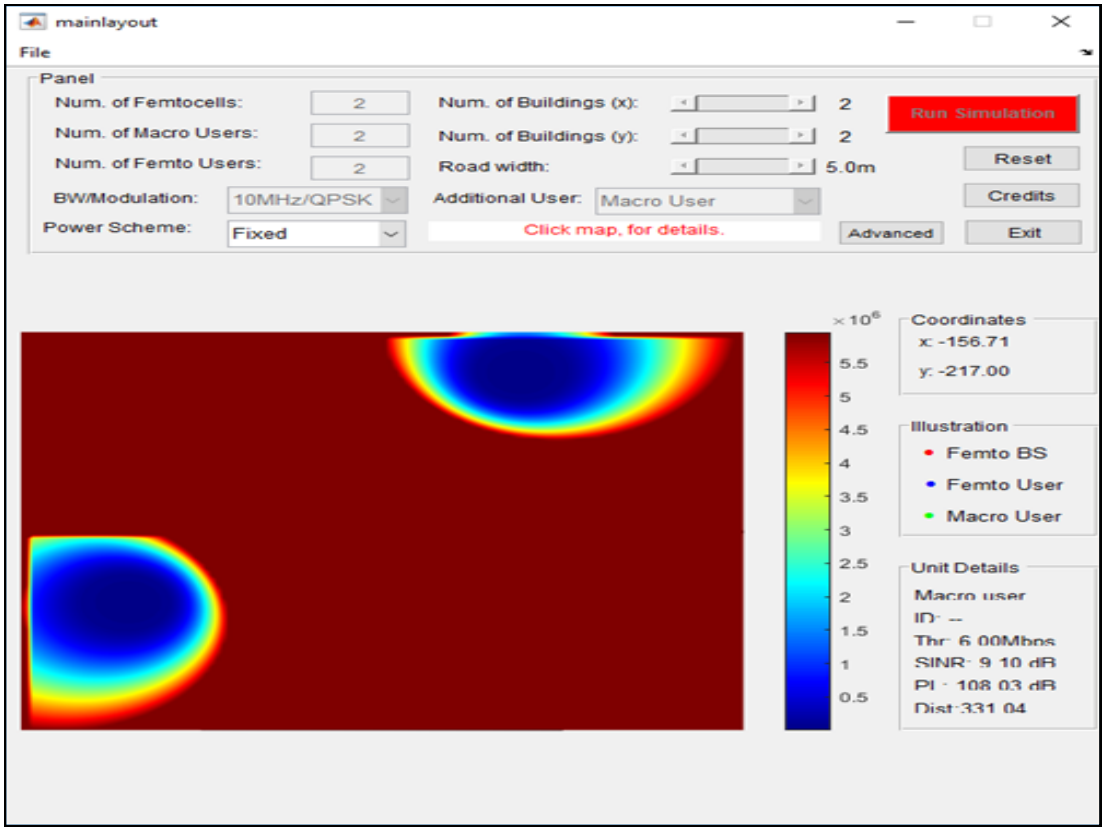

Figure 5.6. The signal strength display for LTE-A HetNet

6. CONCLUSIONS AND FUTURE DIRECTIONS

The Heterogeneous Network (HetNet) has emerged as one of the most promising developments toward achieving the target of the Long Term Evolution-Advanced (LTE-A) systems. However, Co Channel Interference (CCI) is one of the critical challenges of HetNet, that degrades the overall performance of a system. Therefore, an appropriate Radio Resource Management (RRM) mechanism is required to deploy and expand the HetNets properly.

In this thesis, we focus on three different approaches to reduce the effects of CCI and increase the overall capacity of the LTE-A HetNet systems. In Chapter 3, a new FFR scheme has been proposed, which improved the overall throughput of the LTE-A HetNet by controlling the CCI. The total available bandwidth has been divided into seven subbands, which were then allocated to macrocells and femtocells in different zones of the macrocell coverage areas. In order to implement our new approach for frequency reuse, we proposed a so called FFR-3SL algorithm, which tried to find the best available subband for a newly deployed femtocell in a macrocell coverage area. Moreover, in order to verify the accuracy of the proposed method, a Monte Carlo simulation has implemented. Simulation results confirmed that the proposed FFR-3SL method reduced not only the CCI but also improved the throughput and efficiency of the overall system. Furthermore, effect of the UEs resource demand, user density distribution, and variation in the central layer radius on the system performance were investigated and compared with the existing FFR methods. Simulation results show that the proposed approach FFR-3SL outperformed the other FFR approaches for all considered cases.

In Chapter 4, the effect of ULD and user density on our proposed FFR-3SL method had been investigated. The method in this case has been referred to as FFR-3SLU. In FFR-3SLU method, the total available bandwidth is divided into seven subbands while the size of a subband depends on the UEs demand and density in a layer. Hence, the

overall throughput of the LTE-A HetNet system could be improved by managing the radio resources properly. The simulation results showed, that the assignment of a bigger chunk of a subband to the high density user areas achieved higher throughput and better efficiency.

In Chapter 5, the power control algorithm has been presented for the radio resource management (RRM) in LTE-A femtocells network. A simulator tool has been implemented to analyze the SINR and RSRP of the signal. The LTE-A macrocell and femtocell positions were rearranged according to the defined topology for generating the required results. Based on these outcomes and system information, the throughput at UE has calculated to control the connectivity. Furthermore, it was analyzed that PCA method, had the capability to reduce the interference issue due to the unorganized deployment of HetNets.

In the future work model of the system will be extended to investigate the new strategies for RRM in LTE-A femtocells networks. Some of the approaches include fractional frequency reuse and self-organizing methods in femtocells overlay.

In future, a well-organized femtocells deployment strategy will be considered in order to increase the system performance in LTE-A HetNet. Additionally, the Multiple Input Multiple Output (MIMO) beamforming and spatial diversity techniques will be used to mitigate the cross-tier interference and achieve higher throughput. Moreover, Machine Learning (ML) concept will be employed to train the system to efficiently allocate the radio resources in LTE-A HetNet.

REFERENCES

[1] Morley J., Widdicks K. and Hazas M., Digitalisation, energy and data demand: The impact of Internet traffic on overall and peak electricity consumption, *Energy Research & Social Science*, 2018**, 38**(1), 128–137.

[2] Cisco VNI96, Cisco Visual Networking Index: Global Mobile Data Traffic Forecast, *Cisco White Paper*, 2019**, 1**(1), 1–10.

[3] Conti M., Li Q. Q., Maragno A. and Spolaor R., The dark side channel of mobile devices: A survey on network traffic analysis, *IEEE Communications Surveys and Tutorials*, 2018**, 20**(4), 2658–2713.

[4] Kukushkin A., *4G-Long Term Evolution (LTE) System*, 2nd ed., Wiley Telecom, 2018.

[5] Elnashar A. and El-Saidny M. A., *LTE and LTE-A Overview*, Wiley Telecom, 2018.

[6] Liu X., Initial Study on the Architecture of Field Observation in 5G Era, *2018 IEEE 5G World Forum (5GWF), IEEE*, 524–527, Silicon Valley, CA, USA, July 2018.

[7] Usama M. and Erol-Kantarci M., A Survey on Recent Trends and Open Issues in Energy Efficiency of 5G, *Sensors*, 2019**, 19**(14), 3126.

[8] Yousefi Z. H. and Albanna A., Capacity augmentation of 3G cellular networks, a deep learning approach, *University of California*, 2019**, 1**(1), 1–8.

[9] Peng M., Li Y., Zhao Z. and Wang C., System architecture and key technologies for 5G heterogeneous cloud radio access networks, *IEEE network*, 2015**, 29**(2), 6–14.

[10] Ali M. S., An overview on interference management in 3GPP LTE-advanced heterogeneous networks, *International Journal of Future Generation Communication and Networking*, 2015**, 8**(1), 55–68.

[11] Wang Y. and Chien K., EPS: energy-efficient pricing and resource scheduling in LTE-A heterogeneous networks, *IEEE Transactions on Vehicular Technology*, 2018**, 67**(9), 8832–8845.

[12] Ahmed R., Malviya A. K., Kaur M. J. and Mishra V. P., Comprehensive Survey of Key Technologies Enabling 5G-IoT, *Proceedings of 2nd International Conference on Advanced Computing and Software Engineering (ICACSE) 2019, Elsevier*, Sultanpur, UP, India, Apr. 2019.

[13] Akpakwu G. A., Silva B.. J., Hancke G. P. and Abu-Mahfouz A. M., A survey on 5G networks for the Internet of Things: Communication technologies and challenges, *IEEE Access*, 2017**, 6**(4), 3619–3647.

[14] Agiwal M., Roy A. and Saxena N., Next generation 5G wireless networks: A comprehensive survey, *IEEE Communications Surveys & Tutorials*, 2016**, 18**(3), 1617–1655.

[15] Al-Turjman F., 5G-enabled devices and smart-spaces in social-IoT: an overview, *Future Generation Computer Systems*, 2019**, 92**(1), 732–744.

[16] Paradisi A., Yacoub M. D., Figueiredo F. L. and Tronco T., *Long Term Evolution: 4G and Beyond*, Springer, 2015.

[17] Haidine A., Aqqal A. and Ouahmane H., Modeling the migration of mobile networks towards 4G and beyond, *Proceedings of the Mediterranean Conference on Information & Communication Technologies 2015*, 355–363, 2016.

[18] Krishna M. B. and Mauri J. L., *Advances in Mobile Computing and Communications*, CRC Press, 2016.

[19] Dixit S., Katiyar H. and Singh A. K., Energy-Efficient Design of LTE Systems, *Strategic Innovations and Interdisciplinary Perspectives in Telecommunications and Networking*, IGI Global, India, 84–96, 2019.

[20] Gomez C. K., Goratti L., Rasheed T., Boru D., Fedrizzi R. and Riggio R., *The evolutionary role of communication technologies in public safety networks*, ISTE Press, 2015.

[21] Carrillo D., De-Figueiredo F. A., Figueiredo F. . and Miranda J., LTE and Beyond, *Long Term Evolution*, Springer, 1–25, 2016.

[22] Aziz O. A., Empirical Stairwell Propagation Models for Long Term Evolution Applications, PhD thesis, Universiti Teknologi Malaysia, 2016.

[23] Moghaddam S. S., *Cognitive Radio in 4G/5G Wireless Communication Systems*, BoD–Books on Demand, 2018.

[24] Alencar M. S. and Da-Rocha J., Long-Term Evolution, *Communication Systems*, Springer, 283–302, 2020.

[25] Delson T. and Jose I., A Survey on 5G Standards, Specifications and Massive MIMO Testbed Including Transceiver Design Models Using QAM Modulation Schemes, *2019 International Conference on Data Science and Communication (IconDSC), IEEE*, 1–7, Bangalore, India, India, Mar. 2019.

[26] Ibrahim L. F., Salman H. A., Taha Z. F., Akkari N., Aldabbagh G. and Bamasak O., A survey on heterogeneous mobile networks planning in indoor dense areas, *Personal and Ubiquitous Computing*, 2019**, 1**(1), 1–12.

[27] Safdar G. A., Interference Mitigation in Cognitive Radio-Based LTE Femtocells, *LTE Communications and Networks: Femtocells and Antenna Design Challenges*, 2018**, 1**(1), 30–38.

[28] Huq K., Busari S. A., Rodriguez J., Frascolla V., Bazzi W. and Sicker D. C., Terahertz-Enabled Wireless System for Beyond-5G Ultra-Fast Networks: A Brief Survey, *IEEE Network*, 2019**, 33**(4), 89–95.

[29] Collins M. ve diğ., 5g mobile promises to connect and speed up everything, *Equity*, 2019**, 33**(4), 6.

[30] Cisco V., Cisco Visual Networking Index Forecast and Trends, *White Paper*, Cisco Inc., 1–30, 2018.

[31] Zayas A. D., Pérez C. A. G., Pérez M. R. and Merino P., 3GPP evolution on LTE connectivity for IoT, *Integration, Interconnection, and Interoperability of IoT Systems*, Springer, 1–20, 2018.

[32] Laselva D., Lopez P. D., Rinne M. and Henttonen T., 3GPP LTE-WLAN aggregation technologies: functionalities and performance comparison, *IEEE Communications Magazine*, 2018**, 56**(3), 195–203.

[33] Hoglund A., Van D. P., Tirronen T., Liberg O., Sui Y. and Yavuz E. A., 3GPP Release 15 Early Data Transmission, *IEEE Communications Standards Magazine*, 2018**, 2**(2), 90–96.

[34] Rajoria S., Trivedi A. and Godfrey W., A comprehensive survey: Small cell meets massive MIMO, *Physical communication*, 2018**, 26**(1), 40–49.

[35] Wang Y and Pedersen K. I., Performance analysis of enhanced inter-cell interference coordination in LTE-Advanced heterogeneous networks, *2012 IEEE 75th Vehicular Technology Conference (VTC Spring), IEEE*, 1–5, Yokohama, Japan, May 2012.

[36] Damnjanovic A., Montojo J., Cho J., Ji H., Yang J. and Zong P., UE's role in LTE advanced heterogeneous networks, *IEEE Communications Magazine*, 2012**, 50**(2), 164–176.

[37] Anpalagan A., Bennis M. and Vannithamby R., *Design and deployment of small cell networks*, Cambridge University Press, 2015.

[38] Radwan A. and Rodriguez J., *Energy Efficient Smart Phones for 5G Networks*, Springer, 2014.

[39] Lopez-Perez D., Guvenc I. and Chu X., Mobility management challenges in 3GPP heterogeneous networks, *IEEE Communications Magazine*, 2012**, 50**(12), 70–78.

[40] Damnjanovic A., Montojo J., Wei Y., Ji T., Luo T., Vajapeyam M., Yoo T., Song O. and Malladi D., A survey on 3GPP heterogeneous networks, *IEEE Wireless communications*, 2011**, 18**(3), 10–21.

[41] Hasan M., Ismail A., Aisha H., Abdullah K., Ramli H., Islam S., Nafi N. and Mohamad H., Inter-cell interference coordination in Heterogeneous Network: A qualitative and quantitative analysis, *2013 IEEE 11th Malaysia International Conference on Communications (MICC), IEEE*, 361–366, Kuala Lumpur, Malaysia, Nov. 2013.

[42] Mahmud A., Lin Z. and Hamdi K. A., On the energy efficiency of fractional frequency reuse techniques, *2014 IEEE Wireless Communications and Networking Conference (WCNC), IEEE*, 2348–2353, 2014.

[43] Ali N. A., El-Dakroury M. A, El-Soudani M., ElSayed H. M., Daoud R. M. and Amer H. H., New hybrid frequency reuse method for packet loss minimization in LTE network, *Journal of advanced research*, 2015**, 6**(6), 949–955.

[44] Chang H. and Rubin I., Optimal downlink and uplink fractional frequency reuse in cellular wireless networks, *IEEE Transactions on Vehicular Technology*, 2015**, 65**(4), 2295–2308.

[45] Chen C., Videv S., Tsonev D. and Haas H., Fractional frequency reuse in DCO-OFDM-based optical attocell networks, *Journal of Lightwave Technology*, 2015**, 33**(19), 3986–4000.

[46] Kawser M. T., Islam M. R., Ahmed K. I., Karim M. R. and Saif J. B., Efficient Resource Allocation and Sectorization for Fractional Frequency Reuse (FFR) in LTE Femtocell Systems. *Radioengineering*, 2015**, 24**(4), 1–8.

[47] Kumar S., Kalyani S. and Giridhar K., Impact of Sub-Band Correlation on SFR and Comparison of FFR and SFR, *IEEE Transactions on Wireless Communications*, 2016**, 15**(8), 5156–5166.

[48] Gupta S., Kumar S., Zhang R., Kalyani S., Giridhar K. and Hanzo L., Resource allocation for D2D links in the FFR and SFR aided cellular downlink, *IEEE Transactions on Communications*, 2016**, 64**(10), 4434–4448.

[49] Li Y., Niu C., Ye F. and Hu R. Q., A universal frequency reuse scheme in LTE-A heterogeneous networks, *Wireless Communications and Mobile Computing*, 2016**, 16**(17), 2839–2851.

[50] Garcıa-Morales J., Femenias G. and Riera-Palou F., Statistical analysis and optimization of a fifth-percentile user rate constrained design for FFR/SFR-aided OFDMA-based cellular networks, *IEEE Transactions on Vehicular Technology*, 2017**, 67**(4), 3406–3419.

[51] Onu C., Salihu B. and Abolarinwa J., Enhanced Fractional Frequency Reuse in Lte-A Heterogeneous OFDMA Network, *ATBU Journal of Science, Technology and Education*, 2018**, 6**(2), 18–27.

[52] Saquib N., Hossain E. and Kim D. I., Fractional frequency reuse for interference management in LTE-advanced hetnets, *IEEE Wireless Communications*, 2013**, 20**(2), 113–122.

[53] Fradi N., Najeh S. and Boujemaa H., Resource allocation in OFDMA networks with femto and macro-cells coexistence using Fractional Frequency Reuse (FFR), *Fourth International Conference on Communications and Networking, ComNet-2014, IEEE*, 1–5, Hammamet, Tunisia, Mar. 2014.

[54] Davaslioglu K., Coskun C. C. and Ayanoglu E., Energy-efficient resource allocation for fractional frequency reuse in heterogeneous networks, *IEEE Transactions on Wireless Communications*, 2015**, 14**(10), 5484–5497.

[55] Lee P., Lee T., Jeong J. and Shin J., Interference management in LTE femtocell systems using fractional frequency reuse, *2010 The 12th international conference on advanced communication technology (ICACT)*, vol. 2*, IEEE*, 1047–1051, Phoenix Park, South Korea, Feb. 2010.

[56] Clerckx B., Lozano A., Sesia S., Van R. C. and Papadias C. B., *3GPP lte and lte-advanced*, Nature Publishing Group, 2009.

[57] Roth J., Tummala M., McEachen J. and Scrofani J., Quantifying location privacy in urban next-generation cellular networks, *Proceedings of the 51st Hawaii International Conference on System Sciences*, Hawaii, 2018.

[58] Mishra D. and Mishra A., Self-optimization in LTE: An Approach to Reduce Call Drops in Mobile Network, *International Conference on Futuristic Trends in Network and Communication Technologies, Springer*, 382–395, 2018.

[59] Yahya A., Introduction to LTE Cellular Networks, *LTE-A Cellular Networks*, Springer, 1–4, 2017.

[60] Dehghani M., Arshad K. and MacKenzie R., LTE-Advanced radio access enhancements: A survey, *Wireless Personal Communications*, 2015**, 80**(3), 891–921.

[61] Arafat A. O., Al-Hourani A., Nafi N. S. and Gregory M. A., A survey on dynamic spectrum access for LTE-advanced, *Wireless Personal Communications*, 2017**, 97**(3), 3921–3941.

[62] Wang H. and Fapojuwo A. O., A survey of enabling technologies of low power and long range machine-to-machine communications, *IEEE Communications Surveys & Tutorials*, 2017**, 19**(4), 2621–2639.

[63] Seo H., Lee K., Yasukawa S., Peng Y. and Sartori P., LTE evolution for vehicle-to-everything services, *IEEE communications magazine*, 2016**, 54**(6), 22–28.

[64] Kassim M., Rahman R. A., Aziz M. A., Idris A. and Yusof M. I., Performance analysis of VoIP over 3G and 4G LTE network, *2017 International Conference on Electrical, Electronics and System Engineering (ICEESE), IEEE*, 37–41, Kanazawa, Japan, Nov. 2017.

[65] Singh R. K. and Singh R., 4G LTE cellular technology: Network architecture and mobile standards, *International Journal of Emerging Research in Management &Technology*, 2016**, 5**(12), 70–90.

[66] Ndujiuba C. U., Oni O. and Ibhaze A. E., Comparative analysis of digital modulation techniques in LTE 4G systems, *Journal of wireless Networking and Communications*, 2015**, 5**(2), 60–66.

[67] Sharma S. and Singh H., Comparison of Different Digital Modulation Techniques in LTE System using OFDM AWGN Channel: A Review, *International Journal of Computer Applications*, 2016**, 143**(3), 105–150.

[68] Guo Y., Research on Key Technologies of 4G-LTE Uplink Physical Link, *Proceedings of the 2016 2nd International Conference on Materials Engineering and Information Technology Applications (MEITA 2016)*, Atlantis Press, 2017.

[69] Navita A., Performance analysis of OFDMA, MIMO and SC-FDMA technology in 4G LTE networks, *Proceeding of th 6th International Conference on Cloud Syststem and Big Data Engineering*, 554–558, Noida, India, July 2016.

[70] Bujunuru A., Priyanka M. and Charan K. P., OFDM Synthetic Aperture Radar Imaging with Sufficient Cyclic Prefix, *International Journal of Engineering Technology Science and Research*, 2017**, 4**(9), 340–344.

[71] Abdoli J., Jia M. and Ma J., Filtered OFDM: A new waveform for future wireless systems, *2015 IEEE 16th International Workshop on Signal Processing Advances in Wireless Communications (SPAWC), IEEE*, 66–70, Stockholm, Sweden, July 2015.

[72] Al-jzari A. A., Kostanic I. and Mabrok K. H. M., Effect of variable cyclic prefix length on OFDM system performance over different wireless channel models, *Univers. J. Commun. Networ*, 2015**, 3**(1), 7–14.

[73] Sharma S., Sharma E. B. and Kanwar V., Review Paper on Performance of OFDM in 4g Wireless Communication, *International Journal*, 2016**, 6**(9), 1–20.

[74] Muhammad Asshad, Sajjad Ahmad Khan, Adnan Kavak and Kerem Küçük, Evaluation of Multi Dual-Hop and Cooperative Relay Networks using MGF Based Analysis, *2019 1st International Informatics and Software Engineering Conference (UBMYK), IEEE*, 1–4, Ankara, Turkey, Nov. 2019.

[75] Muhammad Asshad, Sajjad Ahmad Khan, Adnan Kavak and Kerem Küçük, Performance Analysis of Multi-Node Cooperative Network with Amplify and Forward Relay Protocol, *2019 1st International Informatics and Software Engineering Conference (UBMYK), IEEE*, 1–4, 2019.

[76] Furht B. and Ahson S. A., *Long Term Evolution: 3GPP LTE radio and cellular technology*, Crc Press, 2016.

[77] Singh R. K. and Singh R., 4G LTE cellular technology: Network architecture and mobile standards, *International Journal of Emerging Research in Management &Technology*, 2016**, 5**(12), 100–115.

[78] Ali M. S., An overview on interference management in 3GPP LTE-advanced heterogeneous networks, *International Journal of Future Generation Communication and Networking*, 2015**, 8**(1), 55–68.

[79] Ye Y., Wu D., Shu Z. and Qian Y., Overview of LTE spectrum sharing technologies, *IEEE Access*, 2016**, 4**(2), 8105–8115.

[80] Cui H., Leung V. C., Li S. and Wang X., LTE in the unlicensed band: Overview, challenges, and opportunities, *IEEE Wireless Communications*, 2017**,** **24**(4), 99–105.

[81] Damnjanovic A., Montojo J., Wei Y., Ji T., Luo T., Vajapeyam M., Yoo T., Song O. and Malladi D., A survey on 3GPP heterogeneous networks, *IEEE Wireless communications*, 2011**,** **18**(3), 10–21.

[82] Wu G., Mizuno M. and Havinga P. J., MIRAI architecture for heterogeneous network, *IEEE Communications Magazine*, 2002**,** **40**(2), 126–134.

[83] Su G., Li L., Lin X. and Wang H., On the optimal small cell deployment for energy-efficient heterogeneous cellular networks, *2014 Sixth International Conference on Ubiquitous and Future Networks (ICUFN), IEEE*, 172–175, Shanghai, China, July 2014.

[84] Nasser N., Hasswa A. and Hassanein H., Handoffs in fourth generation heterogeneous networks, *IEEE Communications Magazine*, 2006**,** **44**(10), 96–103.

[85] Cerwall P., Jonsson P., Möller R., Bävertoft S., Carson S. and Godor I., *Ericsson mobility report*, Ericsson, 2015.

[86] Zhou Y., Yu F. R., Chen J. and Kuo Y., Resource allocation for information-centric virtualized heterogeneous networks with in-network caching and mobile edge computing, *IEEE Transactions on Vehicular Technology*, 2017**,** **66**(12), 11339–11351.

[87] Hasan M., Ismail A., Abdalla A. H., Abdullah K., Ramli H., Islam S. and Saeed R. A., Inter-cell interference coordination in LTE-A HetNets: A survey on self organizing approaches, *2013 International Conference on Computing, Electrical and Electronic Engineering (ICCEEE), IEEE*, 196–201, Khartoum, Sudan, Aug. 2013.

[88] Sajjad Ahmad Khan, Sultan Aldırmaz Çolak, Adnan Kavak and Kerem Kücük, A User Location Distribution Based FFR Strategy for Efficient Utilization of Radio Resources in LTE-A HetNets, *2019 1st International Informatics and Software Engineering Conference (UBMYK), IEEE*, 1–6, 2019.

[89] Yaacoub E., Green 5G femtocells for supporting indoor generated IoT traffic, *Internet of Things (IoT) in 5G Mobile Technologies*, Springer, 129–152, 2016.

[90] Park E., del-Pobil A. and Kwon S., The role of internet of things (IoT) in smart cities: Technology roadmap-oriented approaches, *Sustainability*, 2018**,** **10**(5), 1388.

[91] Hernández A., Guıo I. and Valdovinos A., Radio resource allocation for interference management in mobile broadband OFDMA based networks, *Wireless Communications and Mobile Computing*, 2010**,** **10**(11), 1409–1430.

[92] Khan S. A., Asshad M., Kucuk K. and Kavak A., A Power Control Algorithm (PCA) and Software Tool for Femtocells in LTE-A Networks, *Sakarya University Journal of Science*, 2018**,** **22**(4), 1124–1129.

[93] Zhang L., Yang L. and Yang T., Cognitive interference management for LTE-A femtocells with distributed carrier selection, *2010 IEEE 72nd Vehicular Technology Conference-Fall, IEEE*, 1–5, Ottawa, ON, Canada, Sept. 2010.

[94] Khan S. A., Kavak A., Colak S. A. and Kucuk K., A Novel Fractional Frequency Reuse Scheme for Interference Management in LTE-A HetNets, *IEEE Access*, 2019**, 7**(1), 109662–109672.

[95] Park C. S. and Park S., Analysis of RSRP measurement accuracy, *IEEE Communications Letters*, 2016**, 20**(3), 430–433.

[96] Lee J., Kim Y., Kwak Y., Zhang J., Papasakellariou A., Novlan T., Sun C. and Li Y., LTE-advanced in 3GPP Rel-13/14: An evolution toward 5G, *IEEE Communications Magazine*, 2016**, 54**(3), 36–42.

[97] Abdullahi S. U., Liu J., Huang C. and Zhang X., Enhancing throughput performance in LTE-advanced HetNets with buffered fractional frequency reuse, *2016 Eighth International Conference on Ubiquitous and Future Networks (ICUFN), IEEE*, 918–923, Vienna, Austria, July 2016.

[98] Çakir M. and Kalaycioglu A., Power adjustment based interference management in dense heterogeneous femtocell networks, *2017 2nd International Conference on Computer and Communication Systems (ICCCS), IEEE*, 133–137, Krakow, Poland, July 2017.

[99] Battikh D. B. C., Outage probability formulas for cellular networks: contributions for MIMO, CoMP and time reversal features, PhD thesis, Télécom ParisTech, 2012.

[100] Xu L. and Cao N., A Smart QoE Aware Network Selection Solution for IoT Systems in HetNets Based 5G Scenarios, *2018 International Conference on Cyber-Enabled Distributed Computing and Knowledge Discovery (CyberC), IEEE*, 361–3617, Zhengzhou, China, China, Oct. 2018.

[101] Ahmad I., Kumar T., Liyanage M., Okwuibe J., Ylianttila M. and Gurtov A., Overview of 5G security challenges and solutions, *IEEE Communications Standards Magazine*, 2018**, 2**(1), 36–43.

[102] Geller M. and Nair P., 5G Security Innovation with Cisco, *Whitepaper Cisco Public*, Cisco Inc., 1–29, 2018.

[103] Muhammad Asshad, Adnan Kavak, Kerem Küçük and Sajjad Ahmad Khan, Using Moment Generating Function for Performance Analysis in Non-Regenerative Cooperative Relay Networks with Max-Min Relay Selection, *AEU-International Journal of Electronics and Communications*, 2020**, 1**(1), 1–22.

[104] Al-Turjman F., Ever E. and Zahmatkesh H., Small cells in the forthcoming 5G/IoT: Traffic modelling and deployment overview, *IEEE Communications Surveys & Tutorials*, 2018**, 21**(1), 28–65.

[105] Mandour M., Gebali F., Elbayoumy A. D., Hamid G. M. A. and Abdelaziz A., Handover Optimization and User Mobility Prediction in LTE Femtocells Network, *2019 IEEE International Conference on Consumer Electronics (ICCE), IEEE*, 1–6, Las Vegas, NV, USA, USA, Jan. 2019.

[106] Asshad M., Khan S. A., Kavak A., Küçük K. and Msongaleli D. L., Cooperative communications using relay nodes for next-generation wireless networks with optimal selection techniques: A review, *IEEJ Transactions on Electrical and Electronic Engineering*, 2019**, 14**(5), 658–669.

[107] Yengi Y., Khan S. A. and Küçük K., Design and performance analysis of information centric network for Internet of Things, *2017 25th Signal Processing and Communications Applications Conference (SIU), IEEE*, 1–4, Antalya, Turkey, May 2017.

[108] Khan S. A., Kavak A., Kucuk K. and Asshad M., A New Fractional Frequency Reuse Method for Interference Management in LTE-A HetNets, *2019 27th Signal Processing and Communications Applications Conference (SIU), IEEE*, 1–4, Sivas, Turkey, Apr. 2019.

[109] Hassan H., Ahmed I., Ahmad R., Khammari H., Bhatti G., Ahmed W. and Alam M. M., A Machine Learning Approach to Achieving Energy Efficiency in Relay-Assisted LTE-A Downlink System, *Sensors*, 2019**, 19**(16), 3461.

[110] Abdullahi S. U., Liu J., Huang C. and Zhang X., Enhancing throughput performance in LTE-advanced HetNets with buffered fractional frequency reuse, *2016 Eighth International Conference on Ubiquitous and Future Networks (ICUFN), IEEE*, 918–923, Vienna, Austria, July 2016.

[111] Abuibaid M. A. and Colak S. A., Energy-efficient massive MIMO system: Exploiting user location distribution variation, *AEU-International Journal of Electronics and Communications*, 2017**, 72**(1), 17–25.

[112] Raida V., Svoboda P., Lerch M. and Rupp M., Repeatability for Spatiotemporal Throughput Measurements in LTE, *2019 IEEE 89th Vehicular Technology Conference (VTC2019-Spring), IEEE*, 1–5, Kuala Lumpur, Malaysia, May 2019.

[113] Lee C., Lin J., Wu. C., Lee M. and Yeh F., A dynamic CRE and ABS scheme for enhancing network capacity in LTE-advanced heterogeneous networks, *Wireless Networks*, 2019**, 25**(6), 3307–3322.

[114] Zarrinkoub H., *Understanding LTE with MATLAB: from mathematical modeling to simulation and prototyping*, John Wiley & Sons, 2014.

[115] Radio F. R., Requirements for LTE Pico eNodeB, tech. rep.*, 3GPP TR 36.931*, 2016.

[116] Osterhage W., *Wireless Network Security*, CRC Press, 2018.

[117] Chang C., Srirama S. N. and Buyya R., Internet of Things (IoT) and New Computing Paradigms, *Fog and Edge Computing: Principles and Paradigms*, 2019(), 1–23.

[118] Waheidi Y. M., Jubran M. and Hussein M., User Driven Multiclass Cell Association in 5G HetNets for Mobile & IoT Devices, *IEEE Access*, 2019**,** **7**(3), 82991–83000.

PUBLICATIONS

Asshad M., Kavak A., Küçük K., **Khan S. A.**, Using Moment Generating Function for Performance Analysis in Non-Regenerative Cooperative Relay Networks with Max-Min Relay Selection, *AEU International Journal of Electronics and Communications*, 2020, 1–23.

Khan S. A., Kavak A., Çolak S. A. and Küçük K., A Novel Fractional Frequency Reuse Scheme for Interference Management in LTE-A HetNets, *IEEE Access*, 2019, **7**(1), 109662 - 109672.

Asshad M., **Khan S. A.**, Kavak A., Küçük K. and Msongaleli D. L., Cooperative Communications using Relay Nodes for Next-Generation Wireless Networks with Optimal Selection Techniques: A Review, *IEEJ Transaction on Electrical and Electronic Engineering*, 2019, **14**(5), 658-669.

Khan S. A., Asshad M., Küçük K. and Kavak A., A Power Control Algorithm (PCA) and Software Tool for Femtocells in LTE-A Networks, *Sakarya Üniversitesi Fen Bilimleri Enstitüsü Dergisi*, 2018, **22**(4), 1124-1129.

Khan S. A., Kavak A., Küçük K. and Asshad M., A New Fractional Frequency Reuse Method for Interference Management in LTE-A HetNets, *27th Signal Processing and Communications Applications Conference (SIU)*, IEEE, Sivas, Turkey, 24-26 April 2019.

Khan S. A., Sultan A. Ç., Kavak A. and Küçük K., A User Location Distribution Based FFR Strategy for Efficient Utilization of Radio Resources in LTE-A Het-Nets, *International Informatics and Software Engineering Conference (UBMYK)*, IEEE, Ankara, Turkey, 06-07 November 2019.

Asshad M., **Khan S. A.**, Kavak A. and Küçük K., Evaluation of Multi Dual-Hop and Cooperative Relay Networks using MGF Based Analysis, *International Informatics and Software Engineering Conference (UBMYK)*, IEEE, Ankara, Turkey, 06-07 November 2019.

Asshad M., **Khan S. A.**, Kavak A. and Küçük K., Performance Analysis of Multi-Node Cooperative Network with Amplify and Forward Relay Protocol, *International Informatics and Software Engineering Conference (UBMYK)*, IEEE, Ankara, Turkey, 06-07 November 2019.

Yengi Y., **Khan S. A.**, and Küçük K., Design and performance analysis of information centric network for Internet of Things, *25th Signal Processing and Communications Applications Conference (SIU)*, IEEE, Antalya, Turkey, 15-18 May 2017.

Khan S. A., Asshad M., Kavak A., and Küçük K., A novel Radio Resource Management (RRM) technique for Femtocells in LTE-Pro Networks, *International Engineering Research Symposium (UMAS)*, Duzce, Turkey, 11-13 September 2017.

Khan S. A., Kavak A., Asshad M. and Fıdan Kaya., Transmit Power Control (TPC) Algorithm for LTE-A Femtocell Networks, *International Conference on Advanced Technology and Sciences (ICAT)*, Konya, Turkey, 01-03 September 2016.

CURRICULUM VITAE

Sajjad Ahmad Khan received his Bachelor of Science in Information Technology from the University of Engineering and Technology, Peshawar, Pakistan and Master of Science in Telecommunication and Computer Network from IQRA University, Islamabad, Pakistan. He completed his Doctor of Philosophy (PhD) in Computer Engineering at Kocaeli University, Turkey. He is working in the field of wireless communication and networking, his research area includes radio resource management (RRM) and interference management in LTE-A Heterogeneous Networks (HetNets). He is a student member of IEEE.